アダプティブ空間フィルター
Part II
Adaptive beamformers for MEG source-space analysis: Part II

2017-11-02 改訂版

関原謙介

株式会社　シグナルアナリシス

参考書

本スライドは以下の参考書 ”Adaptive Spatial Filters for …”の第4章から第9章までについての解説である.

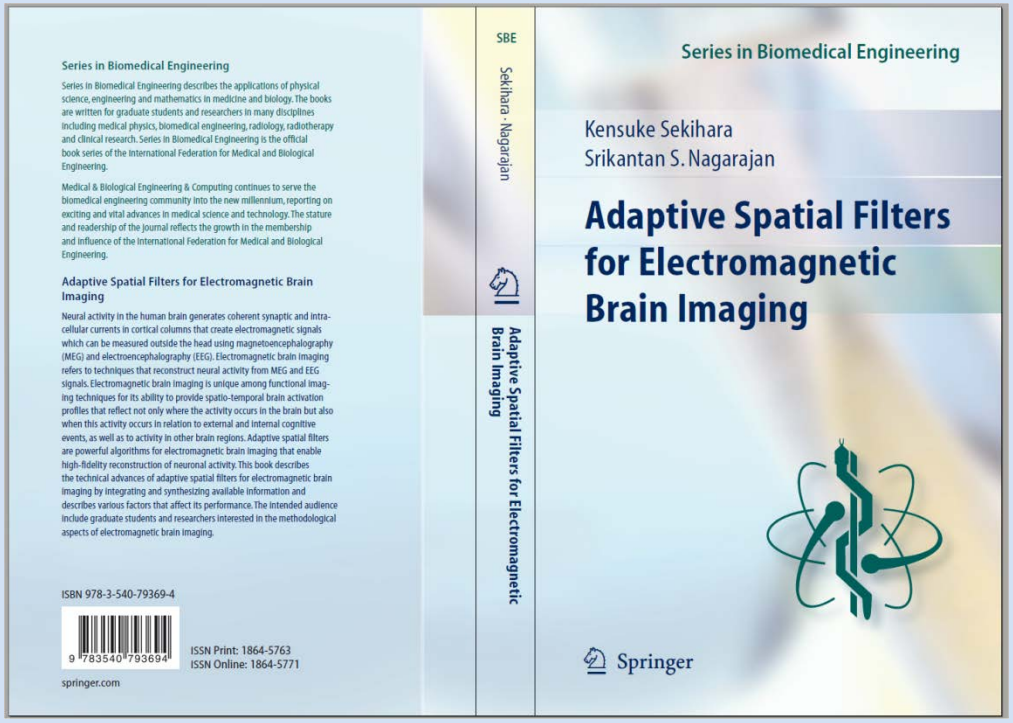

www.electromagneticbrainimaging.info

に正誤表などのこの書籍に対する情報がアップロードされている.

MEGデータの適用に際し生じる問題

Minimum-variance filter

フィルター重み： $$\boldsymbol{w}(\boldsymbol{r}) = \frac{\boldsymbol{R}^{-1}\boldsymbol{l}(\boldsymbol{r})}{\boldsymbol{l}^{T}(\boldsymbol{r})\boldsymbol{R}^{-1}\boldsymbol{l}(\boldsymbol{r})}$$

出力パワー： $$\left\langle \hat{s}(\boldsymbol{r},t)^{2} \right\rangle = \boldsymbol{w}^{T}(\boldsymbol{r})\boldsymbol{R}\boldsymbol{w}(\boldsymbol{r}) = \frac{1}{\boldsymbol{l}^{T}(\boldsymbol{r})\boldsymbol{R}^{-1}\boldsymbol{l}(\boldsymbol{r})}$$

Sarvas公式を使ってリードフィールドを計算する場合，リードフィールドは球中心でゼロとなる．したがって，フィルター重みや出力パワーは球中心で発散してしまう．

↓

Center-of-the-head artifact

センサーアレイ感度の不均一さ，特に，球中心で感度ゼロとなることから生じるアーチファクトへの対応．

Sarvas公式を用いたコンピュータシミュレーション

BTI148チャンネルセンサーアレイ

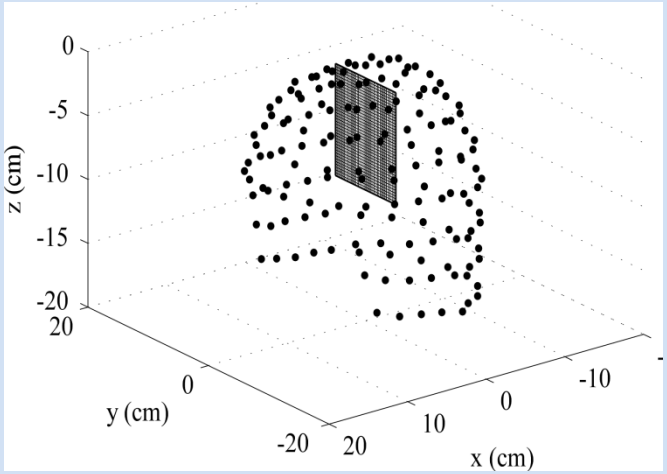

コンピュータシミュレーション：ソース配置

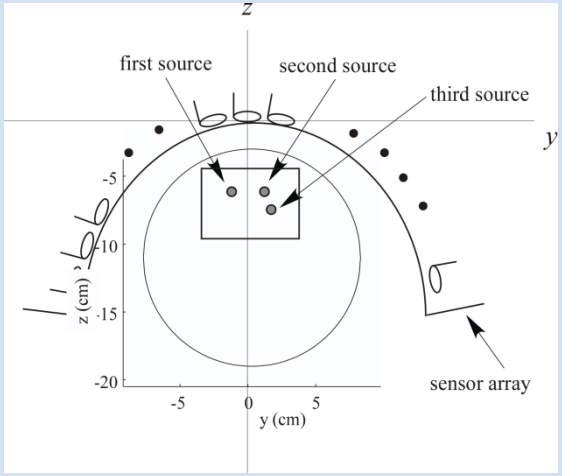

Minimum-variance filterによる再構成結果

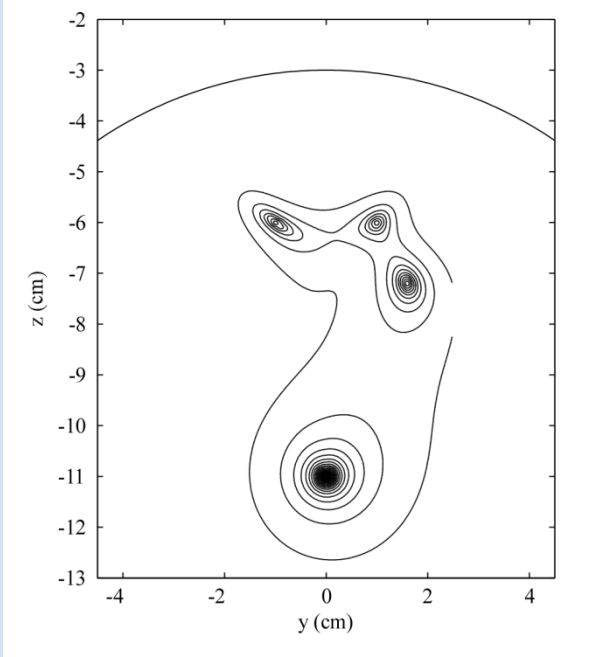

仮定した球中心の位置にアーチファクトを生じる.

解決策1：Array-gain constraint minimum variance filter

$$\boldsymbol{w}(\boldsymbol{r}) = \arg\min_{\boldsymbol{w}} \boldsymbol{w}^T \boldsymbol{R}\boldsymbol{w} \quad \text{subject to} \quad \boldsymbol{w}^T \boldsymbol{l}(\boldsymbol{r}) = \left\| \boldsymbol{l}(\boldsymbol{r}) \right\|$$

空間フィルターのゲインをリードフィールドのノルムに等しくする．$\left\| \boldsymbol{l}(\boldsymbol{r}) \right\|$ は位置 $\boldsymbol{r}$ におけるセンサーアレイのゲインであるので，この制約条件により，センサーのゲインに等しい空間フィルターを求めることになる．

ユニットゲイン制約は，反対に，センサーアレイの感度にかかわらず，フィルターのゲインを１とする方法である．

フィルター重み：
$$\boldsymbol{w}(\boldsymbol{r}) = \frac{\boldsymbol{R}^{-1}\,\tilde{\boldsymbol{l}}(\boldsymbol{r})}{[\tilde{\boldsymbol{l}}^T(\boldsymbol{r})\boldsymbol{R}^{-1}\tilde{\boldsymbol{l}}(\boldsymbol{r})]} \qquad \tilde{\boldsymbol{l}}(\boldsymbol{r}) = \boldsymbol{l}(\boldsymbol{r}) / \left\| \boldsymbol{l}(\boldsymbol{r}) \right\|$$

出力パワー：
$$\left\langle \hat{s}(\boldsymbol{r},t)^2 \right\rangle = \frac{1}{\tilde{\boldsymbol{l}}^T(\boldsymbol{r})\boldsymbol{R}^{-1}\tilde{\boldsymbol{l}}(\boldsymbol{r})} = \frac{\boldsymbol{l}^T(\boldsymbol{r})\boldsymbol{l}(\boldsymbol{r})}{\boldsymbol{l}^T(\boldsymbol{r})\boldsymbol{R}^{-1}\boldsymbol{l}(\boldsymbol{r})}$$

ベクトルソースに対するArray-gain minimum variance filter: Scalar formulation（スカラー型拡張）

$$\boldsymbol{\eta}_{opt} = \arg\max_{\boldsymbol{\eta}} \frac{\boldsymbol{\eta}^T \boldsymbol{L}^T(\boldsymbol{r})\boldsymbol{L}(\boldsymbol{r})\boldsymbol{\eta}}{\boldsymbol{\eta}^T \boldsymbol{L}^T(\boldsymbol{r})\boldsymbol{R}^{-1}\boldsymbol{L}(\boldsymbol{r})\boldsymbol{\eta}}$$ であるので

行列 $\left[\boldsymbol{L}^T(\boldsymbol{r})\boldsymbol{L}(\boldsymbol{r})\right]^{-1}\left[\boldsymbol{L}^T(\boldsymbol{r})\boldsymbol{R}^{-1}\boldsymbol{L}(\boldsymbol{r})\right]$ の最小固有値を λ_{min}

対応する固有ベクトルを $\boldsymbol{u}_{min}$ とすれば:

フィルター重み: $\boldsymbol{w}(\boldsymbol{r}) = \dfrac{\boldsymbol{R}^{-1}\left[\boldsymbol{L}(\boldsymbol{r})\boldsymbol{u}_{\min} \,/\, \left\|\boldsymbol{L}(\boldsymbol{r})\boldsymbol{u}_{\min}\right\|\right]}{\lambda_{\min}}$

出力パワー: $\left\langle \hat{s}(\boldsymbol{r},t)^2 \right\rangle = \dfrac{1}{\lambda_{\min}}$

ベクトルソースに対するArray-gain minimum variance filter: Vector formulation（ベクトル型拡張）

$\boldsymbol{W}(\boldsymbol{r}) = [\boldsymbol{w}_x(\boldsymbol{r}), \boldsymbol{w}_y(\boldsymbol{r}), \boldsymbol{w}_z(\boldsymbol{r})]$ として以下の最適化から重み行列を求める

$$\boldsymbol{W}(\boldsymbol{r}) = \arg\min_{\boldsymbol{W}} \boldsymbol{W}^T(\boldsymbol{r})\boldsymbol{R}\boldsymbol{W}(\boldsymbol{r}) \quad \text{subject to } \boldsymbol{W}^T(\boldsymbol{r})\boldsymbol{L}(\boldsymbol{r}) = \left\|\boldsymbol{L}(\boldsymbol{r})\right\|$$

重み行列: $\boldsymbol{W}(\boldsymbol{r}) = \boldsymbol{R}^{-1}\tilde{\boldsymbol{L}}(\boldsymbol{r})[\tilde{\boldsymbol{L}}^T(\boldsymbol{r})\boldsymbol{R}^{-1}\tilde{\boldsymbol{L}}(\boldsymbol{r})]^{-1}\tilde{\boldsymbol{L}}^T(\boldsymbol{r})$ を得る.

出力パワー:

$$\left\langle s_x(\boldsymbol{r},t)^2\right\rangle + \left\langle s_y(\boldsymbol{r},t)^2\right\rangle + \left\langle s_z(\boldsymbol{r},t)^2\right\rangle = tr[\boldsymbol{W}^T\boldsymbol{R}\boldsymbol{W}]$$
$$= tr\left[\left[\tilde{\boldsymbol{L}}^T(\boldsymbol{r})\boldsymbol{R}^{-1}\tilde{\boldsymbol{L}}(\boldsymbol{r})\right]^{-1}\right]$$

ただし: $\tilde{\boldsymbol{L}}(\boldsymbol{r}) = \boldsymbol{L}(\boldsymbol{r}) / \left\|\boldsymbol{L}(\boldsymbol{r})\right\|$

解決策2：Weight normalized minimum-variance filter

Minimum-variance filterの重みをnormalizeして用いる.

$$\boldsymbol{w}(\boldsymbol{r}) = \frac{\boldsymbol{R}^{-1}\boldsymbol{l}(\boldsymbol{r})}{\boldsymbol{l}^T(\boldsymbol{r})\boldsymbol{R}^{-1}\boldsymbol{l}(\boldsymbol{r})}$$ を用いて $$\hat{s}(\boldsymbol{r},t) = \frac{\boldsymbol{w}^T(\boldsymbol{r})}{\left\|\boldsymbol{w}(\boldsymbol{r})\right\|}\boldsymbol{y}(t)$$ として出力を求める

$$\frac{\boldsymbol{w}(\boldsymbol{r})}{\left\|\boldsymbol{w}(\boldsymbol{r})\right\|} = \frac{\boldsymbol{w}(\boldsymbol{r})}{\sqrt{\boldsymbol{w}^T(\boldsymbol{r})\boldsymbol{w}(\boldsymbol{r})}} = \frac{\boldsymbol{R}^{-1}\boldsymbol{l}(\boldsymbol{r})}{\sqrt{\boldsymbol{l}^T(\boldsymbol{r})\boldsymbol{R}^{-2}\boldsymbol{l}(\boldsymbol{r})}}$$ であるので：

$$\boldsymbol{w}(\boldsymbol{r}) = \frac{\boldsymbol{R}^{-1}\boldsymbol{l}(\boldsymbol{r})}{\sqrt{\boldsymbol{l}^T(\boldsymbol{r})\boldsymbol{R}^{-2}\boldsymbol{l}(\boldsymbol{r})}}$$ として計算したフィルター重みを用いることに等しい

出力パワー： $$\left\langle \hat{s}(\boldsymbol{r},t)^2 \right\rangle = \frac{\boldsymbol{l}^T(\boldsymbol{r})\boldsymbol{R}^{-1}\boldsymbol{l}(\boldsymbol{r})}{\boldsymbol{l}^T(\boldsymbol{r})\boldsymbol{R}^{-2}\boldsymbol{l}(\boldsymbol{r})}$$ と表される.

Weight normalized minimum-variance filter-続き

Weight normalized minimum-variance filterは以下の最適化から導くことができる.

$$\boldsymbol{w}(\boldsymbol{r}) = \underset{\boldsymbol{w}}{\operatorname{argmin}}\ \boldsymbol{w}^T \boldsymbol{R}\boldsymbol{w} \text{ subject to } \boldsymbol{w}^T\boldsymbol{w} = 1$$

そのため，unit noise-gain minimum-variance filterとも呼ばれる.
（世の中では，noise-normalized beamformerと呼ばれる場合もある.）

この空間フィルターはminimum-varianceフィルターと比べて，高い空間分解能を与える. ただし，再構成結果の定量性に不安定さがあり，積極的な使用は進めない.

Signal Processing分野ではBorgiotti-Kaplan beamformerと呼ばれ，古くから知られている.

Borgiotti, G., and L. Kaplan. "Superresolution of uncorrelated interference sources by using adaptive array techniques." *IEEE Transactions on Antennas and Propagation* 27.6 (1979): 842-845.

ベクトルソースに対するWeight normalized minimum-variance filter：Scalar formulation（スカラー型拡張）

$$\boldsymbol{\eta}_{opt} = \arg\max_{\boldsymbol{\eta}} \frac{\boldsymbol{\eta}^T \boldsymbol{L}^T(\boldsymbol{r})\boldsymbol{R}^{-1}\boldsymbol{L}(\boldsymbol{r})\boldsymbol{\eta}}{\boldsymbol{\eta}^T \boldsymbol{L}^T(\boldsymbol{r})\boldsymbol{R}^{-2}\boldsymbol{L}(\boldsymbol{r})\boldsymbol{\eta}}$$ であるので

行列 $\left[\boldsymbol{L}^T(\boldsymbol{r})\boldsymbol{R}^{-1}\boldsymbol{L}(\boldsymbol{r})\right]^{-1}\left[\boldsymbol{L}^T(\boldsymbol{r})\boldsymbol{R}^{-2}\boldsymbol{L}(\boldsymbol{r})\right]$ の最小固有値を λ_{min}

対応する固有ベクトルを $\boldsymbol{u}_{min}$ とすれば：$\boldsymbol{\eta}_{opt} = u_{\min}$ である.

フィルター重み： $$\boldsymbol{w}(\boldsymbol{r}) = \frac{\boldsymbol{R}^{-1}\boldsymbol{L}(\boldsymbol{r})\boldsymbol{u}_{\min}}{\sqrt{\boldsymbol{u}_{\min}^T \boldsymbol{L}^T(\boldsymbol{r})\boldsymbol{R}^{-2}\boldsymbol{L}(\boldsymbol{r})\boldsymbol{u}_{\min}}}$$

出力パワー： $$\left\langle \hat{s}(\boldsymbol{r},t)^2 \right\rangle = \frac{1}{\lambda_{\min}}$$

ベクトルソースに対するWeight normalized minimum-variance filter : Vector formulation（ベクトル型拡張）

以下の最適化を用いる

$$\boldsymbol{w}_x = \underset{\boldsymbol{w}_x}{\operatorname{argmin}}\ \boldsymbol{w}_x^T \boldsymbol{R} \boldsymbol{w}_x \ \text{ subject to } \ \boldsymbol{w}_x^T \boldsymbol{w}_x = 1,\ \boldsymbol{w}_x^T \boldsymbol{l}_y(\boldsymbol{r}) = 0,\ \boldsymbol{w}_x^T \boldsymbol{l}_z(\boldsymbol{r}) = 0$$

$$\boldsymbol{w}_y = \underset{\boldsymbol{w}_y}{\operatorname{argmin}}\ \boldsymbol{w}_y^T \boldsymbol{R} \boldsymbol{w}_y \ \text{ subject to } \ \boldsymbol{w}_y^T \boldsymbol{l}_x(\boldsymbol{r}) = 0,\ \boldsymbol{w}_y^T \boldsymbol{w}_y = 1,\ \boldsymbol{w}_y^T \boldsymbol{l}_z(\boldsymbol{r}) = 0$$

$$\boldsymbol{w}_z = \underset{\boldsymbol{w}_z}{\operatorname{argmin}}\ \boldsymbol{w}_z^T \boldsymbol{R} \boldsymbol{w}_z \ \text{ subject to } \ \boldsymbol{w}_z^T \boldsymbol{l}_x(\boldsymbol{r}) = 0,\ \boldsymbol{w}_z^T \boldsymbol{l}_y(\boldsymbol{r}) = 0,\ \ \boldsymbol{w}_z^T \boldsymbol{w}_z = 1$$

フィルター重み行列は以下で与えられる.

$$[\boldsymbol{w}_x(\boldsymbol{r}), \boldsymbol{w}_y(\boldsymbol{r}), \boldsymbol{w}_z(\boldsymbol{r})] = \boldsymbol{R}^{-1}\boldsymbol{L}(\boldsymbol{r})[\boldsymbol{L}^T(\boldsymbol{r})\boldsymbol{R}^{-1}\boldsymbol{L}(\boldsymbol{r})]^{-1} \begin{bmatrix} 1/\sqrt{\Upsilon_{1,1}} & 0 & 0 \\ 0 & 1/\sqrt{\Upsilon_{2,2}} & 0 \\ 0 & 0 & 1/\sqrt{\Upsilon_{3,3}} \end{bmatrix}$$

ここで, $\boldsymbol{\Upsilon} = [\boldsymbol{L}^T(\boldsymbol{r})\boldsymbol{R}^{-1}\boldsymbol{L}(\boldsymbol{r})]^{-1}[\boldsymbol{L}^T(\boldsymbol{r})\boldsymbol{R}^{-2}\boldsymbol{L}(\boldsymbol{r})][\boldsymbol{L}^T(\boldsymbol{r})\boldsymbol{R}^{-1}\boldsymbol{L}(\boldsymbol{r})]^{-1}$

Sarvas公式を用いたコンピュータシミュレーション

BTI148チャンネルセンサーアレイ

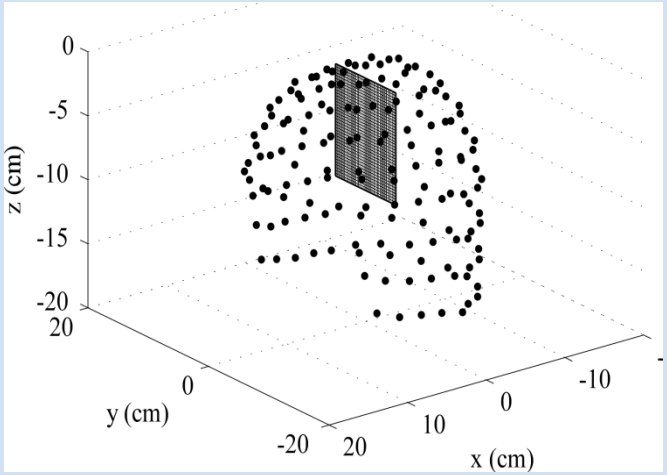

コンピュータシミュレーション：ソース配置

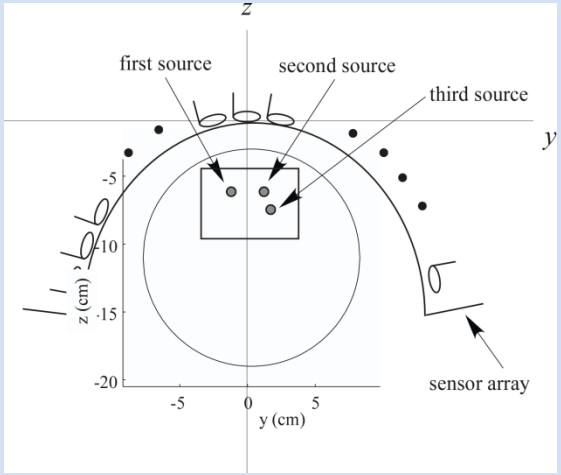

ユニットゲインビームフォーマー

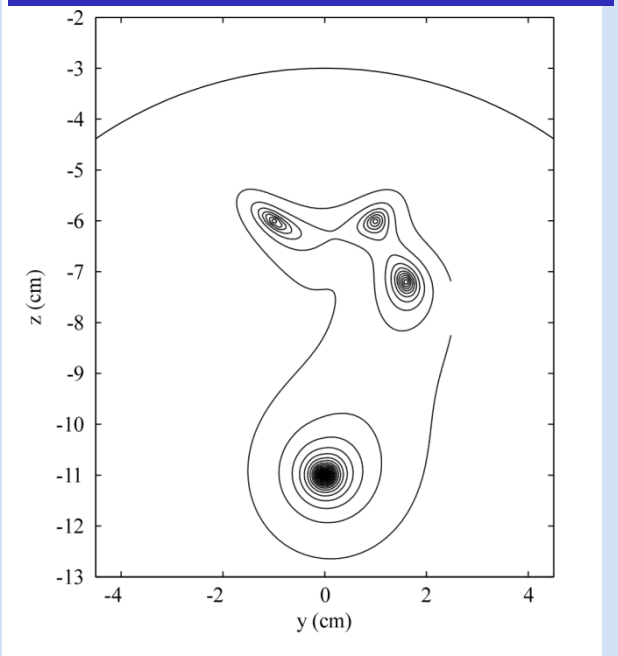

アレイゲインビームフォーマー

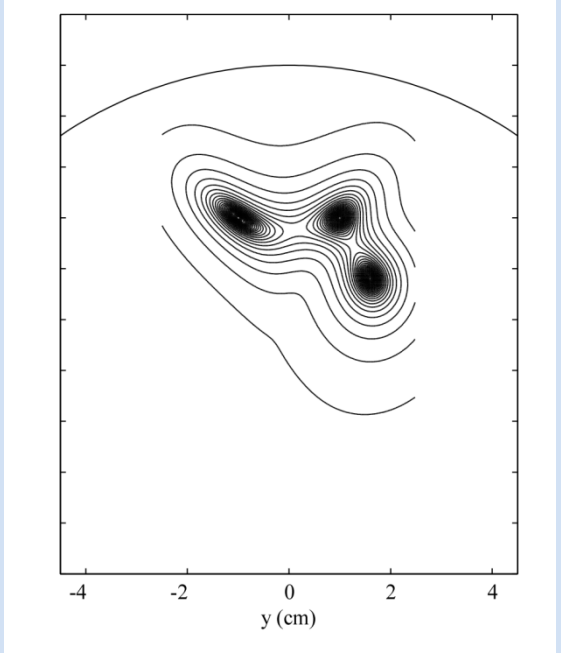

ソース配置

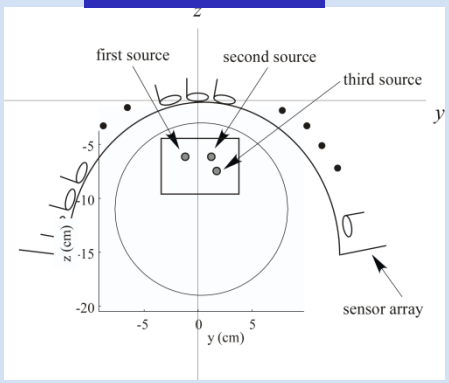

ソースタイムコース

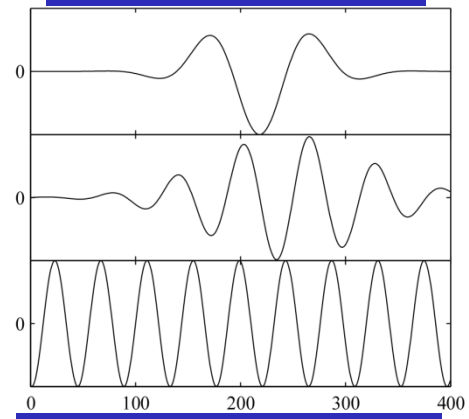

センサータイムコース

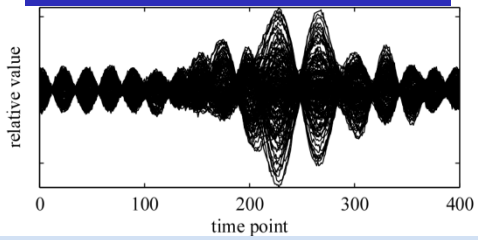

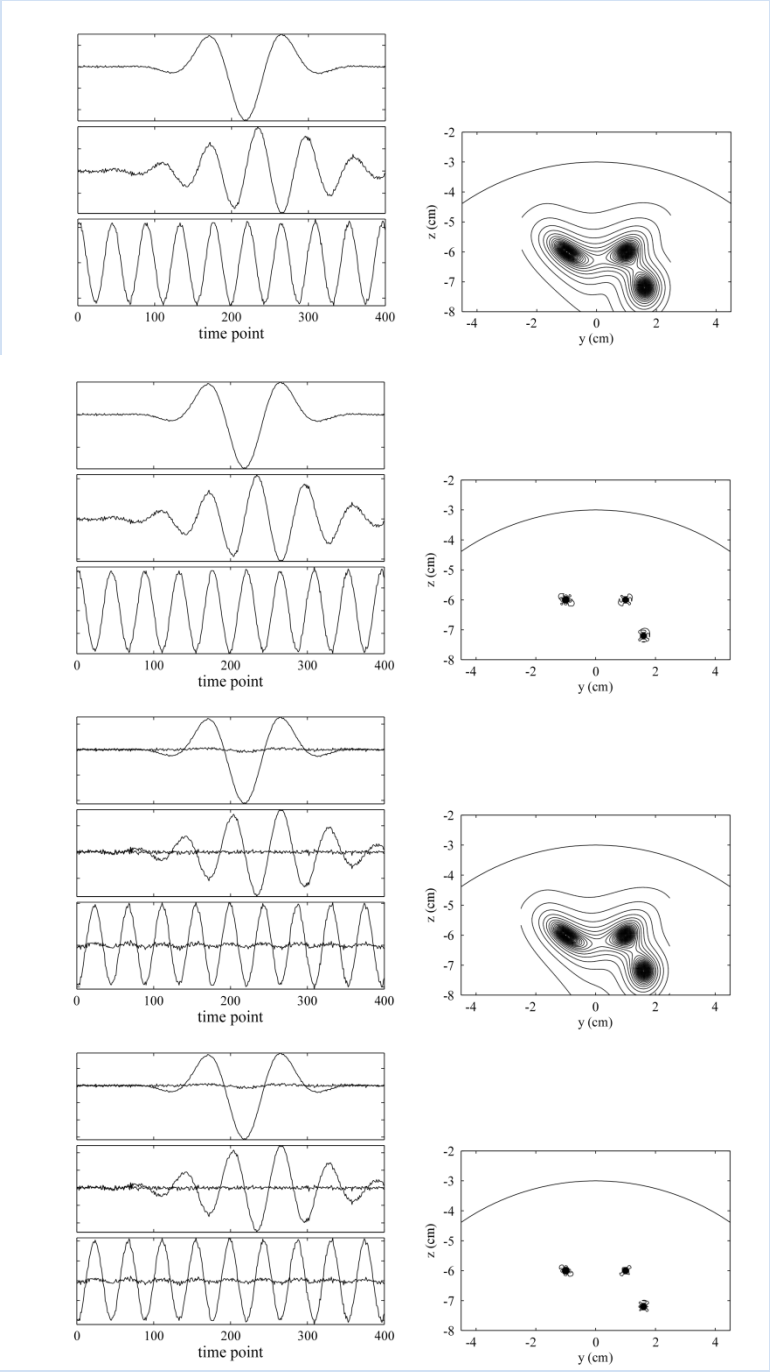

スカラー
アレイゲイン

スカラー
ノイズゲイン

ベクトル
アレイゲイン

ベクトル
ノイズゲイン

補足：再構成結果の次元について

シングルソースの仮定： $\boldsymbol{y}(t) = s(\boldsymbol{r}, t)\boldsymbol{l}(\boldsymbol{r})$

unit-gain filter : $\hat{s}(\boldsymbol{r}, t) = \boldsymbol{w}^T(\boldsymbol{r})\boldsymbol{y}(t) = s(\boldsymbol{r}, t)\boldsymbol{w}^T(\boldsymbol{r})\boldsymbol{l}(\boldsymbol{r}) = s(\boldsymbol{r}, t)$

再構成結果は電流の次元を持つ.

array-gain filter : $\hat{s}(\boldsymbol{r}, t) = \boldsymbol{w}^T(\boldsymbol{r})\boldsymbol{y}(t) = s(\boldsymbol{r}, t)\boldsymbol{w}^T(\boldsymbol{r})\boldsymbol{l}(\boldsymbol{r}) = s(\boldsymbol{r}, t)\left\|\boldsymbol{l}(\boldsymbol{r})\right\|$

再構成結果は磁場の次元を持つ.

unit noise-gain filter :

$$\hat{s}(\boldsymbol{r}, t) = \boldsymbol{w}^T(\boldsymbol{r})\boldsymbol{y}(t) = s(\boldsymbol{r}, t)\frac{\boldsymbol{l}^T(\boldsymbol{r})\boldsymbol{R}^{-1}\boldsymbol{l}(\boldsymbol{r})}{\sqrt{\boldsymbol{l}^T(\boldsymbol{r})\boldsymbol{R}^{-2}\boldsymbol{l}(\boldsymbol{r})}} \approx s(\boldsymbol{r}, t)\left\|\boldsymbol{l}(\boldsymbol{r})\right\|$$

再構成結果は磁場の次元を持つ.

array gain, unit-noise gain filterの再構成結果の解釈について

array-gain filterの再構成結果：$\hat{s}(\boldsymbol{r},t)=s(\boldsymbol{r},t)\left\|\boldsymbol{l}(\boldsymbol{r})\right\|$ はセンサーアレイが検出する磁場強度の「ものさし」で測ったソース強度と解釈できる.

unit noise-gain filterの再構成結果：$\hat{s}(\boldsymbol{r},t)=s(\boldsymbol{r},t)\dfrac{\boldsymbol{l}^T(\boldsymbol{r})\boldsymbol{R}^{-1}\boldsymbol{l}(\boldsymbol{r})}{\sqrt{\boldsymbol{l}^T(\boldsymbol{r})\boldsymbol{R}^{-2}\boldsymbol{l}(\boldsymbol{r})}}$

は，センサーノイズの分散をσ^2として，$\dfrac{1}{\sigma}\hat{s}(\boldsymbol{r},t)=s(\boldsymbol{r},t)\dfrac{\boldsymbol{l}^T(\boldsymbol{r})\boldsymbol{R}^{-1}\boldsymbol{l}(\boldsymbol{r})}{\sigma\sqrt{\boldsymbol{l}^T(\boldsymbol{r})\boldsymbol{R}^{-2}\boldsymbol{l}(\boldsymbol{r})}}$

がフィルタ出力のSN比と解釈できる．したがって，再構成結果 $\hat{s}(\boldsymbol{r},t)/\sigma$ 画像として表示すれば，これは信号源推定のSN比を画像化したものになる．このようにある種の「統計量」を画像化することをStatistical Parametric Mappingと呼ぶ.

ビームフォーマーのベクトル・スカラー型の導出の詳細については，「Adaptive spatial filter..」の第４章に記載がある．また，以下の論文がnoise-gain constraint vector beamformerに関するオリジナル論文である．

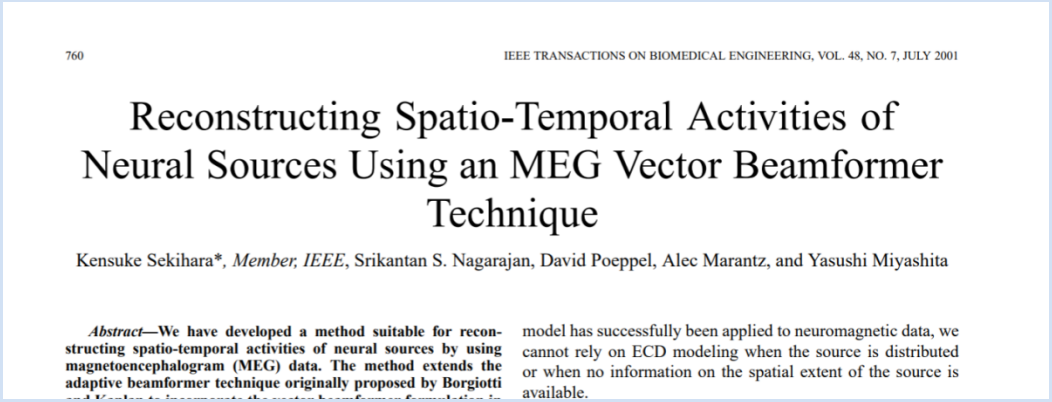

760 IEEE TRANSACTIONS ON BIOMEDICAL ENGINEERING, VOL. 48, NO. 7, JULY 2001

Reconstructing Spatio-Temporal Activities of Neural Sources Using an MEG Vector Beamformer Technique

Kensuke Sekihara*, *Member, IEEE*, Srikantan S. Nagarajan, David Poeppel, Alec Marantz, and Yasushi Miyashita

***Abstract*—We have developed a method suitable for reconstructing spatio-temporal activities of neural sources by using magnetoencephalogram (MEG) data. The method extends the adaptive beamformer technique originally proposed by Borgiotti**

model has successfully been applied to neuromagnetic data, we cannot rely on ECD modeling when the source is distributed or when no information on the spatial extent of the source is available.

また，スカラー型ビームフォーマーについては以下の論文が最初の提案である．

Biomag 96: Proceedings of the Tenth International Conference on Biomagnetism, C. J. Aine eds. Feb. 1996, Page(s): 338-341, Springer-Verlag, New York.

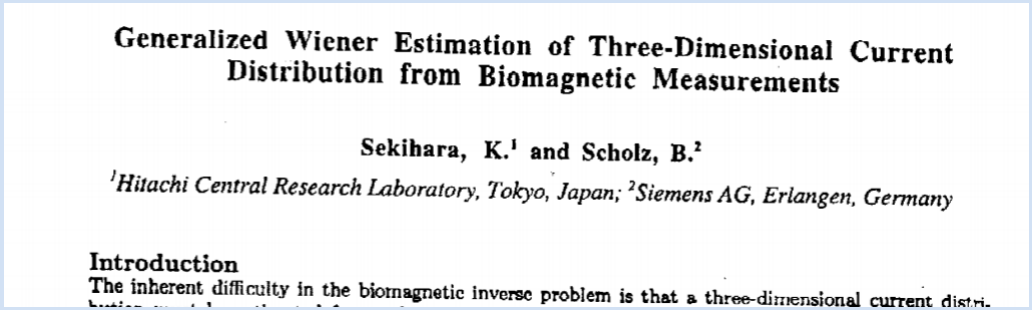

Generalized Wiener Estimation of Three-Dimensional Current Distribution from Biomagnetic Measurements

Sekihara, K.[1] and Scholz, B.[2]

[1]Hitachi Central Research Laboratory, Tokyo, Japan; [2]Siemens AG, Erlangen, Germany

Introduction

The inherent difficulty in the biomagnetic inverse problem is that a three-dimensional current distri-

環境ノイズ(low-rank interference)，およびブレインノイズ(high-rank interference)のビームフォーマー出力への影響

Performance degradation due to interferences

Measurements in non-idealistic, real-life conditions contains various types of interferences.

Beamformerに対するinterference（干渉信号）の影響を議論する.

2種類の干渉信号について議論する

- Low-rank interferences
- High-rank interferences

Low-rank interference

人工的な原因で発生する干渉信号

External disturbance with artificial origins

- Power-line leakage
- Additive base-line drift
- Artificial noise from electrical appliances

⋮

⇓

modeled as low rank signals

このような妨害信号の振る舞いは少数の“固有成分”によって記述できる

Low-rank interference—further assumptions

信号磁場　　干渉・妨害信号

Additivity: $$\boldsymbol{y}(t) = \sum_{q=1}^{Q} \boldsymbol{l}(\boldsymbol{r}_q) s_q(t) + \boldsymbol{\varepsilon} + \boldsymbol{d}(t)$$

Covariance matrix relationship

Total covariance

No correlation: $$\boldsymbol{R} = \boldsymbol{R}_{S+\varepsilon} + \boldsymbol{R}_D$$

Interference covariance

Signal-plus-sensor-noise covariance

$$\boldsymbol{R}_D = \left\langle \boldsymbol{d}(t)\boldsymbol{d}^T(t) \right\rangle$$

$$\boldsymbol{R}_D = \sum_{j=1}^{P_D} \lambda_j \boldsymbol{u}_j \boldsymbol{u}_j^T$$

When $\boldsymbol{R}_D \propto \boldsymbol{u}\boldsymbol{u}^T$（$\boldsymbol{R}_D$をランク1の行列と仮定）

Spatial-filter outputs:

$$\hat{s}(\boldsymbol{r},t) = \frac{\boldsymbol{l}^T(\boldsymbol{r})\boldsymbol{R}^{-1}\boldsymbol{y}(t)}{\boldsymbol{l}^T(\boldsymbol{r})\boldsymbol{R}^{-1}\boldsymbol{l}(\boldsymbol{r})} = \frac{\boldsymbol{l}^T(\boldsymbol{r})(\boldsymbol{R}_{S+\varepsilon}+\boldsymbol{R}_D)^{-1}\boldsymbol{y}(t)}{\boldsymbol{l}^T(\boldsymbol{r})(\boldsymbol{R}_{S+\varepsilon}+\boldsymbol{R}_D)^{-1}\boldsymbol{l}(\boldsymbol{r})}$$

$$= \sum_{q=1}^{Q} s_q(t)\frac{\boldsymbol{l}^T(\boldsymbol{r})\boldsymbol{R}_{S+\varepsilon}^{-1}\boldsymbol{l}(\boldsymbol{r}_q)}{\boldsymbol{l}^T(\boldsymbol{r})\boldsymbol{R}_{S+\varepsilon}^{-1}\boldsymbol{l}(\boldsymbol{r})} \underbrace{\frac{\left[1-\dfrac{\cos(\boldsymbol{l}(\boldsymbol{r}),\boldsymbol{u}\mid\boldsymbol{R}_{S+\varepsilon}^{-1})\cos(\boldsymbol{u},\boldsymbol{l}(\boldsymbol{r}_q)\mid\boldsymbol{R}_{S+\varepsilon}^{-1})}{\cos(\boldsymbol{l}(\boldsymbol{r}),\boldsymbol{l}(\boldsymbol{r}_q)\mid\boldsymbol{R}_{S+\varepsilon}^{-1})}\right]}{\left[1-\cos^2(\boldsymbol{l}(\boldsymbol{r}),\boldsymbol{u}\mid\boldsymbol{R}_{S+\varepsilon}^{-1})\right]}}_{\text{This part is equal to 1}}$$

(when $\boldsymbol{u}$ is very different from $\boldsymbol{l}(\boldsymbol{r})$)

$$\approx \frac{\boldsymbol{l}^T(\boldsymbol{r})\boldsymbol{R}_{S+\varepsilon}^{-1}\boldsymbol{y}(t)}{\boldsymbol{l}^T(\boldsymbol{r})\boldsymbol{R}_{S+\varepsilon}^{-1}\boldsymbol{l}(\boldsymbol{r})}$$

↑

Spatial-filter outputs when the interference does not exist

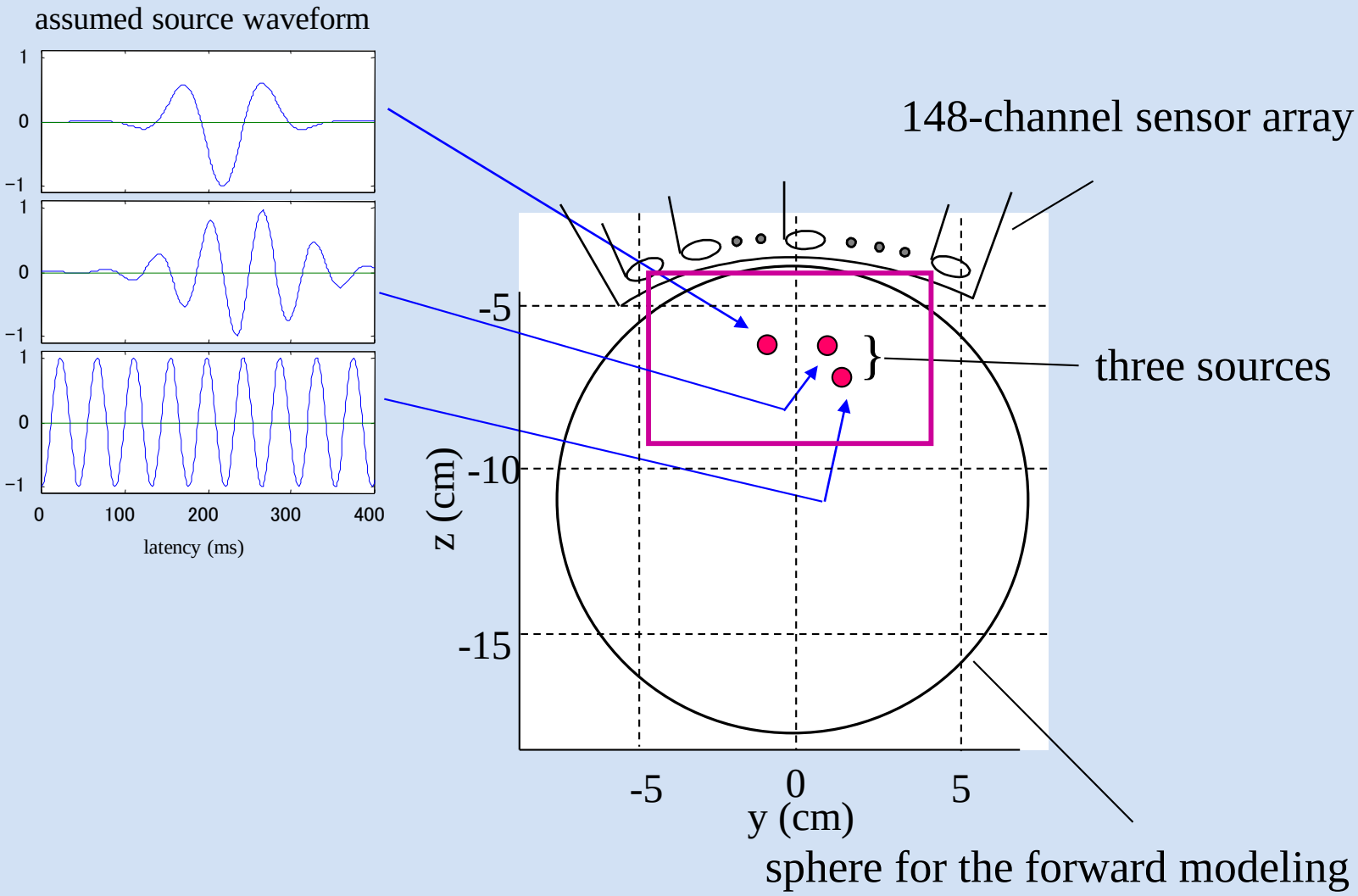
assumed source waveform
1
0
−1
1
0
−1
1
0
−1
0
100
200
300
400
latency (ms)
148-channel sensor array
three sources
-5
-10
-15
z (cm)
-5
0
5
y (cm)
sphere for the forward modeling

Simulated magnetic recordings

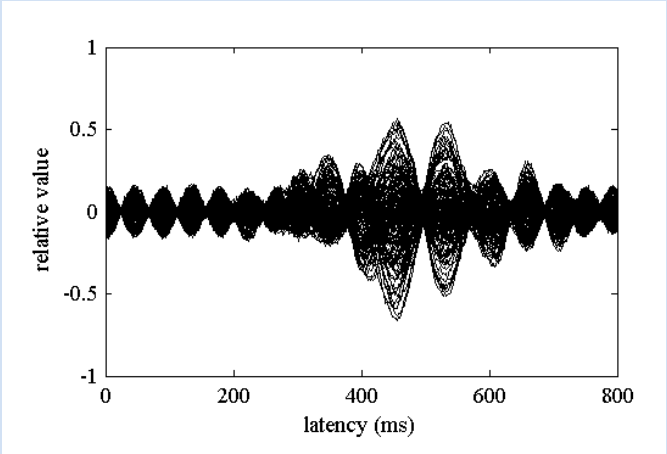

No interference

Periodic interference

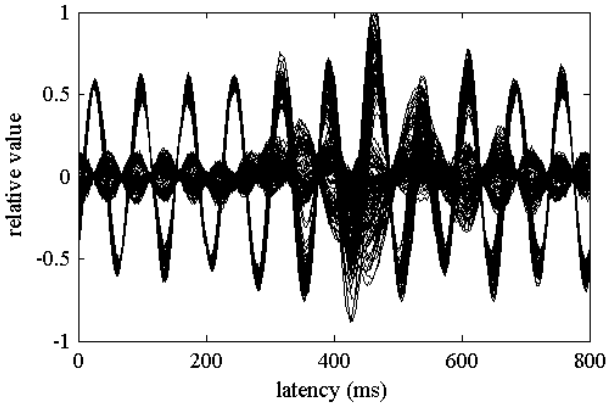

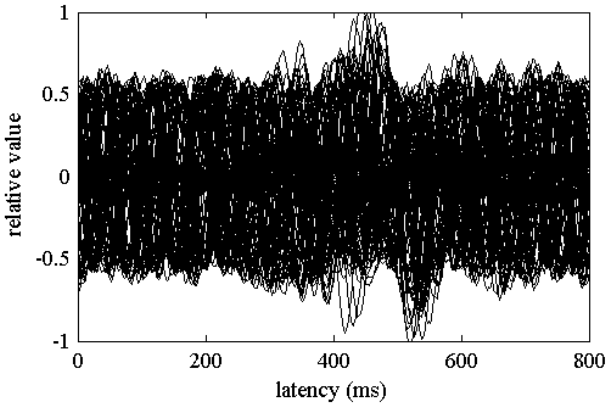

Periodic interference with random phases

Linear trend with random inclinations

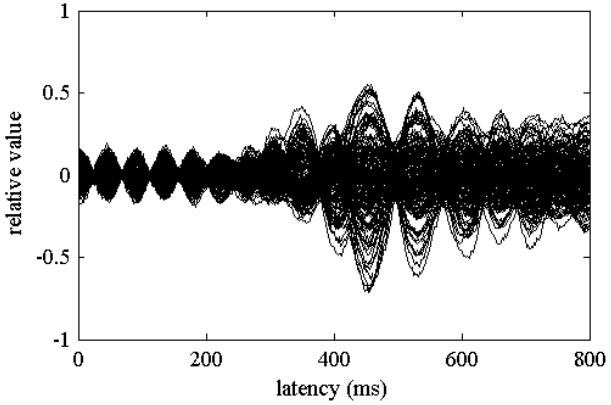

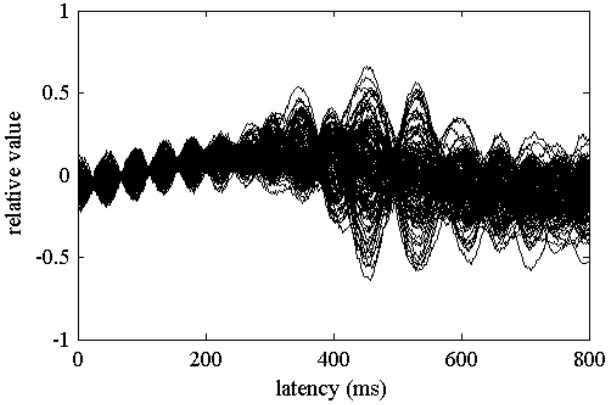

Random linear trend with slow wave activity

Visualization of the first eigenvectors of the interferences

typical lead field of a brain source

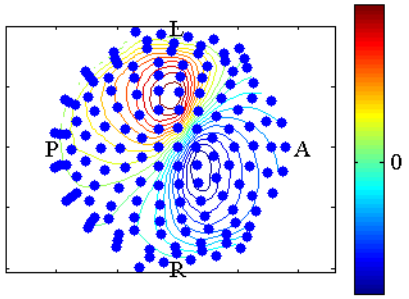

Periodic interference

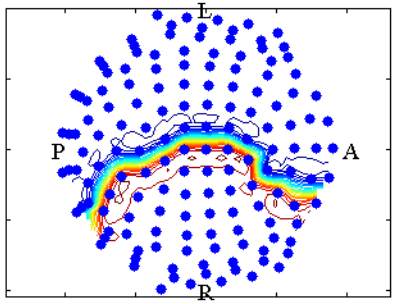

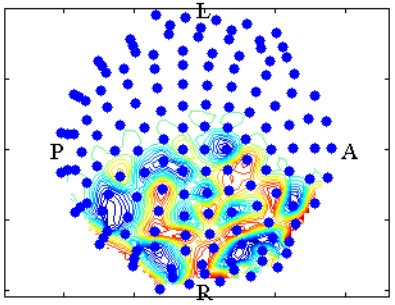

Periodic interference with random phases

Linear trend with random inclinations

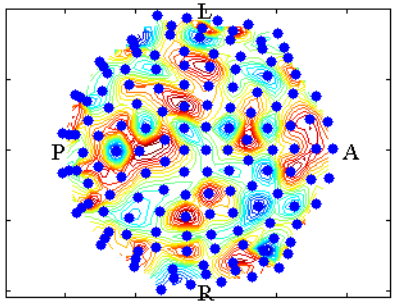

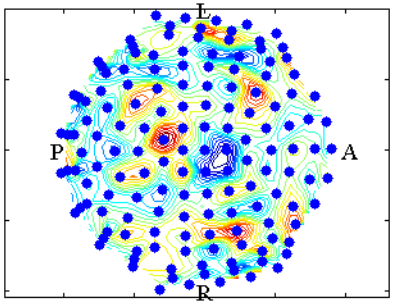

Random linear trend with slow wave activity

Reconstruction results

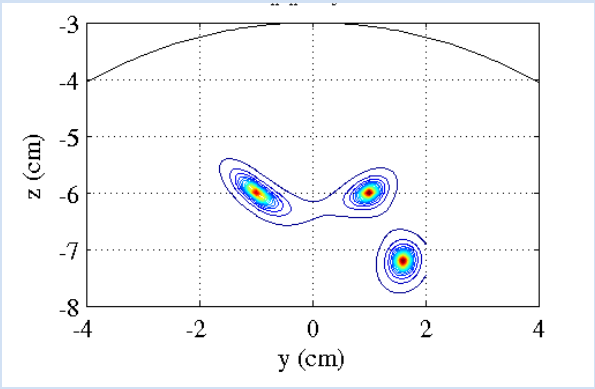

No disturbance

Periodic interference

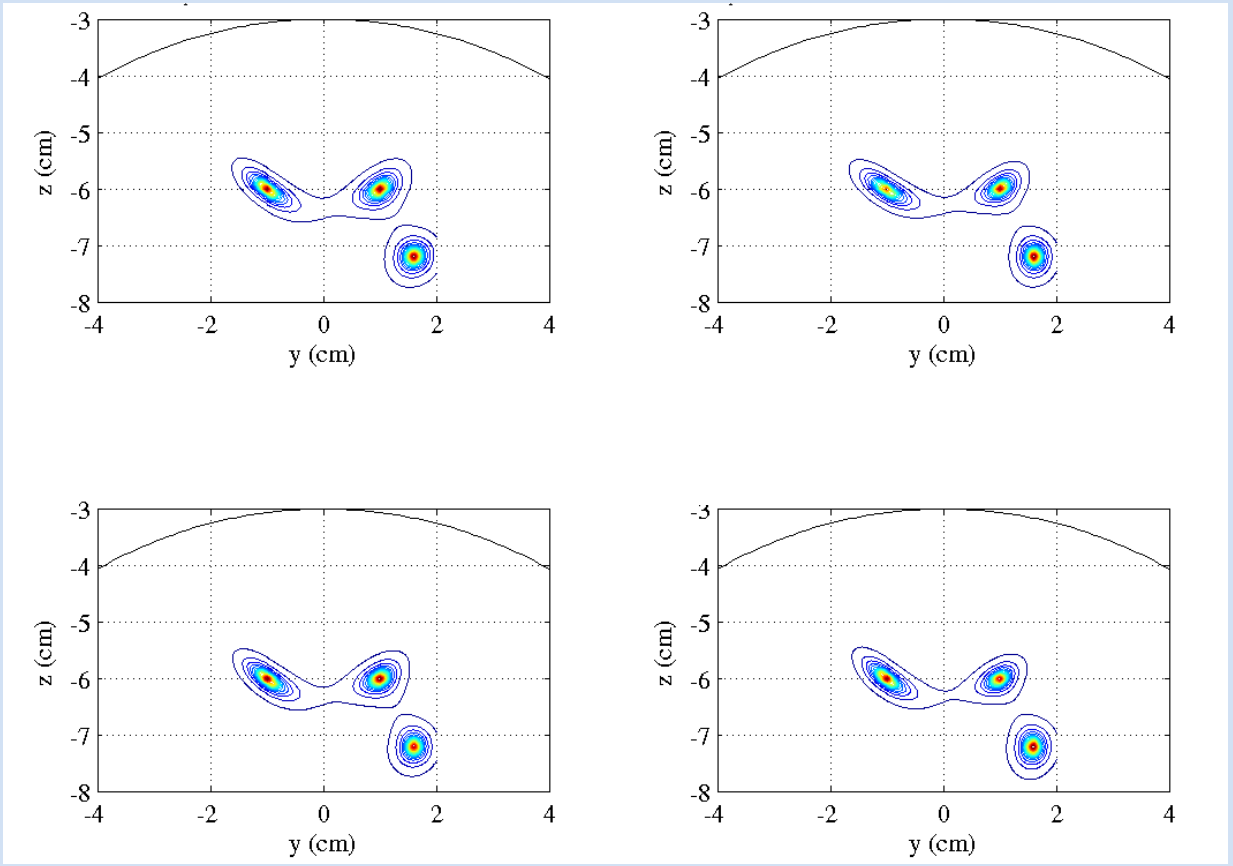

Periodic interference with random phases

Linear trend with random inclinations

Random linear trend with slow wave activity

Reconstructed time courses

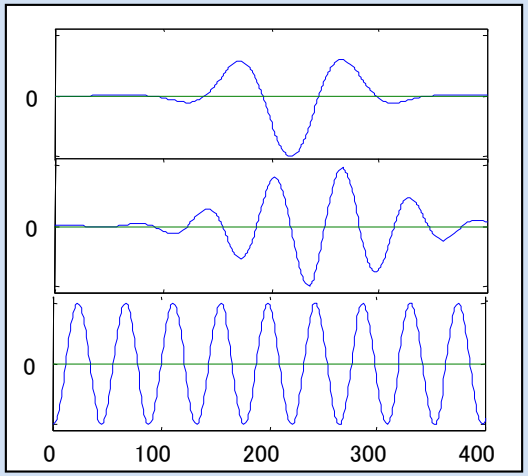

No disturbance

Periodic interference

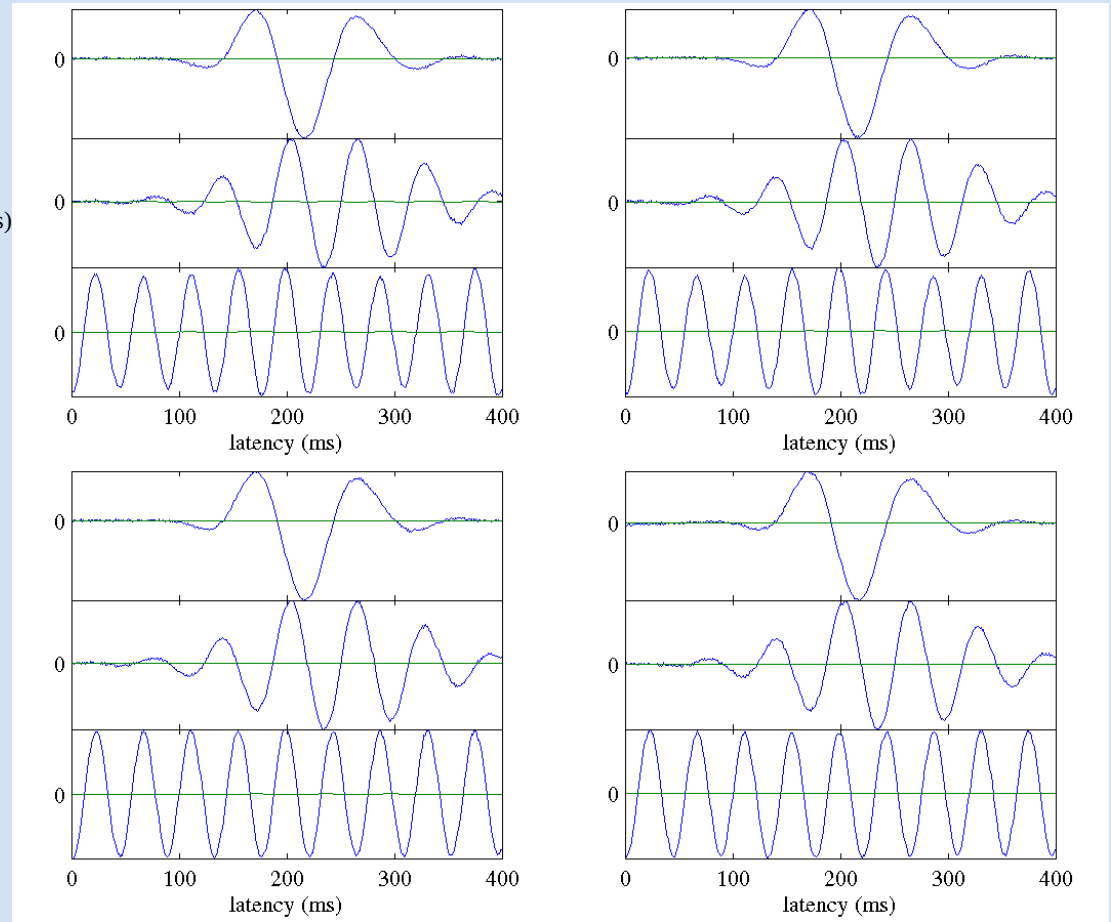

Periodic interference with random phases

Linear trend with random inclinations

Random linear trend with slow wave activity

NeuroImage 50 (2010) 1578–1588

Contents lists available at ScienceDirect

NeuroImage

journal homepage: www.elsevier.com/locate/ynimg

Optimized beamforming for simultaneous MEG and intracranial local field potential recordings in deep brain stimulation patients

Vladimir Litvak [a,*], Alexandre Eusebio [a], Ashwani Jha [a], Robert Oostenveld [b], Gareth R. Barnes [a], William D. Penny [a], Ludvic Zrinzo [a], Marwan I. Hariz [a], Patricia Limousin [a], Karl J. Friston [a], Peter Brown [a]

[a] UCL Institute of Neurology, Queen Square, WC1N 3BG, London, UK
[b] Donders Institute for Brain, Cognition and Behaviour, Radboud University, Nijmegen, The Netherlands

ARTICLE INFO

Article history:
Received 20 November 2009
Revised 23 December 2009
Accepted 24 December 2009
Available online 4 January 2010

ABSTRACT

Insight into how brain structures interact is criti
architectures and may lead to better diagnosis a
simultaneously, magnetoencephalographic (MEG)
Parkinson's disease (PD) patient with bilateral de
nucleus (STN). These recordings offer a unique
subcortical structures and the neocortex. Howeve
artefacts originated from the percutaneous extens

Application of a Null-Beamformer to Source Localisation in MEG Data of Deep Brain Stimulation

Hamid R. Mohseni*§, Morten L. Kringelbach†§, Penny Probert Smith*, Christine E. Parsons†, Katherine S. Young†, Jonathan A. Hyam§, Patrick M. Schweder§, John F. Stein‡§ and Tipu Z. Aziz‡§
*Institute of Biomedical Engineering, School of Engineering Science, University of Oxford, Oxford, UK
†Department of Psychiatry, University of Oxford, Warneford Hospital, UK
‡University of Oxford, Department of Physiology, Anatomy and Genetics, Parks Road, Oxford, OX1 3PT, UK
§Oxford Functional Neurosurgery, Nuffield Department of Surgery, John Radcliffe Hospital, Headington, Oxford, UK

***Abstract*—In this paper, we present an analysis of magnetoencephalography (MEG) signals from a patient with whole-body chronic pain in order to investigate changes in neural activity induced by DBS. The patient is one of the few cases treated using DBS of the anterior cingulate cortex (ACC). Using MEG to reconstruct the neural activity of interest is challenging because of interference to the signal from the DBS device. We demonstrate that a null-beamformer can be used to localise neural activity despite artefacts caused by the presence of DBS electrodes and stimulus pulses. We subsequently verified the accuracy of our**

artefacts mainly originate from the percutaneous extension wire, made of stainless steel [2], used to connect the electrodes to the battery implanted in the abdominal region. The success of the source localisation of the electrode tips described in Section IV-A suggests that DBS electrodes made of titanium may not interfere with the MEG recording.

To date, there has been paucity of studies investigating the effects of stimulation on brain activity using MEG. In 2007, our group carried out the first MEG study of a patient

Beamformerを用いてDBSを装着した患者の脳磁界からの信号源推定が行われている.

参考文献

Beamformer再構成に対するLow-rank interferenceの影響については「Adaptive spatial filter..」の第7章で議論されている．また，以下がオリジナル論文である．

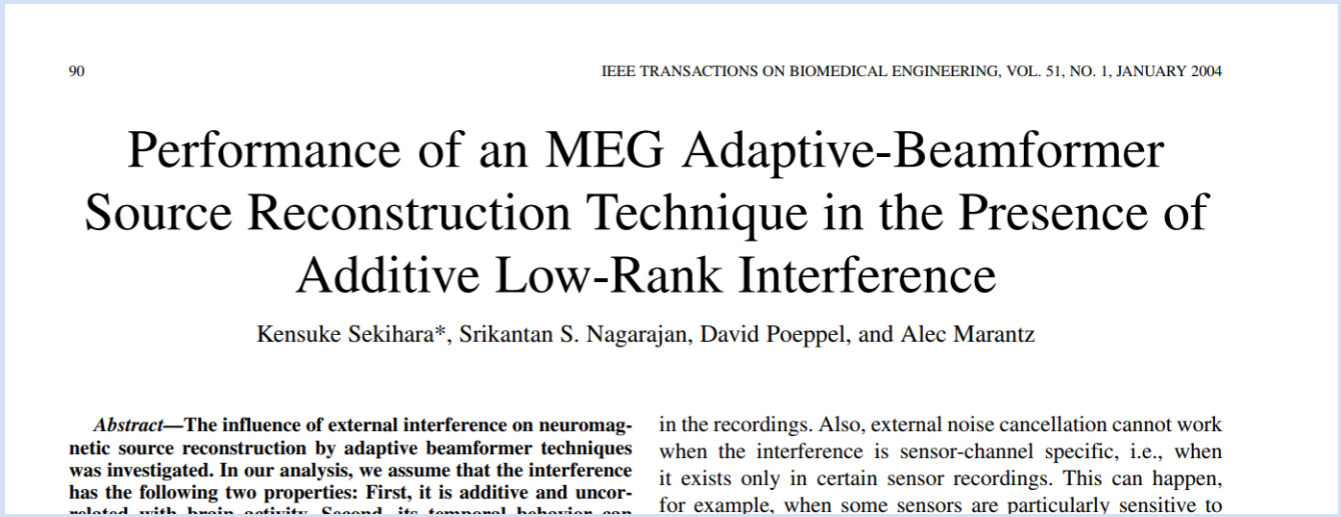

Performance of an MEG Adaptive-Beamformer Source Reconstruction Technique in the Presence of Additive Low-Rank Interference

Kensuke Sekihara*, Srikantan S. Nagarajan, David Poeppel, and Alec Marantz

***Abstract*—The influence of external interference on neuromagnetic source reconstruction by adaptive beamformer techniques was investigated. In our analysis, we assume that the interference has the following two properties: First, it is additive and uncor-**

in the recordings. Also, external noise cancellation cannot work when the interference is sensor-channel specific, i.e., when it exists only in certain sensor recordings. This can happen, for example, when some sensors are particularly sensitive to

High-rank interference

signal source

neurophysiological noise source

$$\boldsymbol{y}(t) = \sum_{j=1}^{P} \boldsymbol{l}(\boldsymbol{r}_j) s(\boldsymbol{r}_j, t) + \sum_{k}^{\infty} \boldsymbol{l}(\boldsymbol{r}_k) \xi(\boldsymbol{r}_k, t) + \boldsymbol{\varepsilon}(t)$$

$\xi(\boldsymbol{r}_k, t)$ 皮質にランダムに分布したインコヒーレントな微弱ソースとしてモデル化できる.

The rank of $\boldsymbol{y}(t)$ is high.

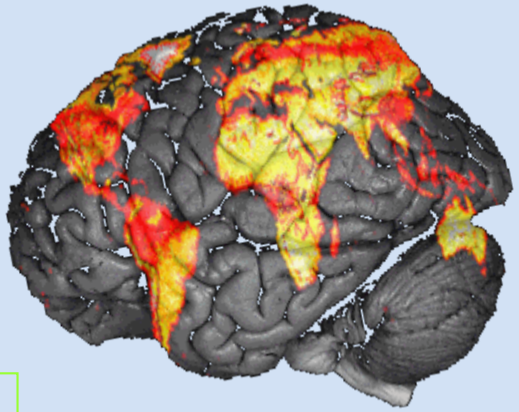

Spontaneous brain activity

•de Munck et al., IEEE Trans. Biomed. Eng., 39, 791-804, 1992.
•Valdes et al., Brain Topography, 4, 309-319, 1992.
•Lutkenhoner, J. Appl. Phys., 75, 7204-7210, 1994.

誘発脳磁界計測に重畳する自発脳磁界はBrain noiseと呼ばれる

Influence of background source activity
(Influence of brain noise)

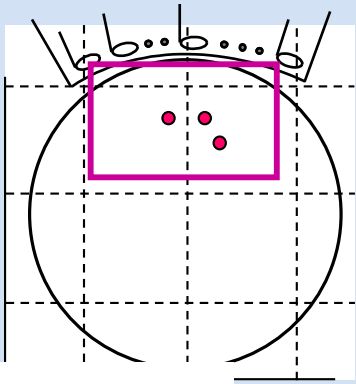

Computer-generated recordings

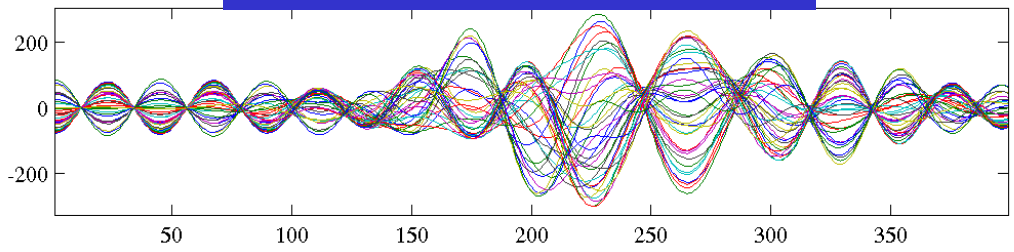

Brain noise

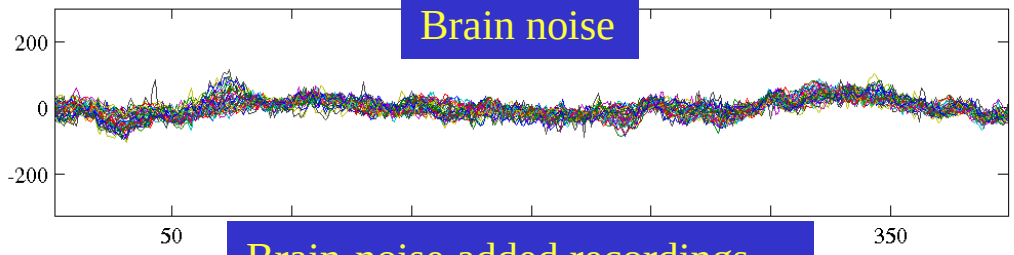

Brain-noise added recordings

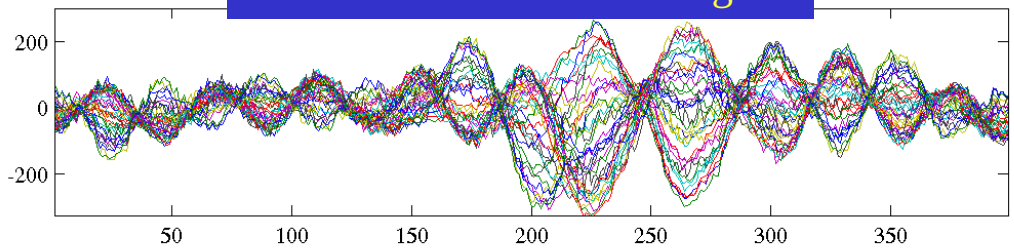

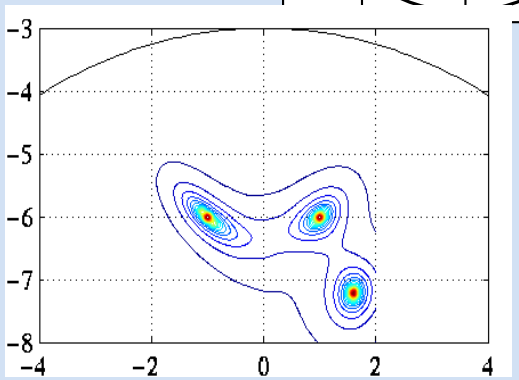

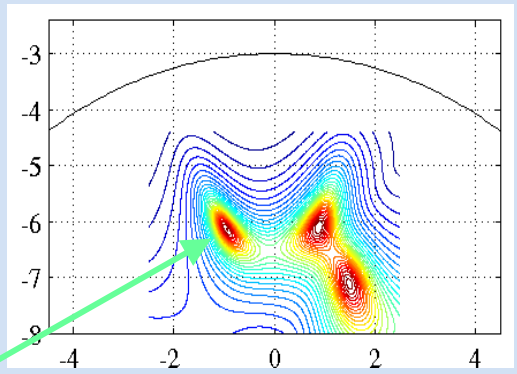

Background activity causes a severe blur.

Dual-condition experiments

Task: $\boldsymbol{y}(t) = \boldsymbol{y}_S(t) + \boldsymbol{y}_I(t) + \boldsymbol{\varepsilon}$

Control: $\boldsymbol{y}_C(t) = \boldsymbol{y}_I(t) + \boldsymbol{\varepsilon}$

↓

Covariance matrix relations

Task: $\boldsymbol{R} = \boldsymbol{R}_S + \boldsymbol{R}_{i+\varepsilon}$

Control: $\boldsymbol{R}_C = \boldsymbol{R}_{i+\varepsilon}$

Problem:

- Brain noiseはソースの存在領域から発生する．除去にはコントロールデータ（Brain noiseのみを含み，関心信号を含まないデータ）が必要である．

Prewhitening estimation of signal covariance

taskとcontrolデータから $\tilde{\boldsymbol{R}} = \boldsymbol{R}_C^{-1/2} \boldsymbol{R} \boldsymbol{R}_C^{-1/2}$ を計算する.

$$\boldsymbol{R} = \boldsymbol{R}_S + \boldsymbol{R}_{i+\varepsilon} \Rightarrow \tilde{\boldsymbol{R}} = \tilde{\boldsymbol{R}}_S + \boldsymbol{I} \Leftarrow$$

この計算をノイズの白色化（prewhitening）と呼ぶ

$\tilde{\boldsymbol{R}}_S$ の固有値展開を $\tilde{\boldsymbol{R}}_S = \sum_{j=1}^{Q} \gamma_j \boldsymbol{u}_j \boldsymbol{u}_j^T$ とすれば，$\tilde{\boldsymbol{R}}$ の固有値展開は：

$$\tilde{\boldsymbol{R}} = \sum_{j=1}^{Q} \gamma_j \boldsymbol{u}_j \boldsymbol{u}_j^T + \sum_{j=Q+1}^{M} \boldsymbol{u}_j \boldsymbol{u}_j^T = \sum_{j=1}^{Q} (\gamma_j + 1) \boldsymbol{u}_j \boldsymbol{u}_j^T .$$

となる．したがって：

$\tilde{\boldsymbol{R}}$ の信号レベル固有値に対する固有ベクトルが $\tilde{\boldsymbol{R}}_S$ の固有ベクトルに等しい

信号レベルとノイズレベル固有値に対する閾値の設定が必要

Prewhitening beamforming

$\tilde{\boldsymbol{R}} = \boldsymbol{R}_C^{-1/2} \boldsymbol{R} \boldsymbol{R}_C^{-1/2}$ を計算する

$\tilde{\boldsymbol{R}}$ の信号レベル固有値に対する固有ベクトルから $\tilde{\boldsymbol{R}}_S$ を推定する：

$$\tilde{\boldsymbol{R}}_S = \sum_{j=1}^{Q} \gamma_j' \boldsymbol{u}_j \boldsymbol{u}_j^T$$

$\tilde{\boldsymbol{R}}_S$ から，prewhiteningの演算を逆に行い $\hat{\boldsymbol{R}}_S$ を推定する：

$$\hat{\boldsymbol{R}}_S = \boldsymbol{R}_C^{1/2} \tilde{\boldsymbol{R}}_S \boldsymbol{R}_C^{1/2} = \boldsymbol{R}_C^{1/2} \left[\sum_{j=1}^{Q} \gamma_j' \boldsymbol{u}_j \boldsymbol{u}_j^T \right] \boldsymbol{R}_C^{1/2}$$

$\hat{\boldsymbol{R}}_S$ を用いてbeamformingを行う：

$$\hat{s}(\boldsymbol{r}, t) = \frac{\boldsymbol{l}^T(\boldsymbol{r}) \hat{\boldsymbol{R}}_S^{-1} \hat{\boldsymbol{y}}_S(t)}{\boldsymbol{l}^T(\boldsymbol{r}) \hat{\boldsymbol{R}}_S^{-1} \boldsymbol{l}(\boldsymbol{r})}; \quad \hat{\boldsymbol{y}}_S(t) = [\boldsymbol{u}_1 \ldots \boldsymbol{u}_Q][\boldsymbol{u}_1 \ldots \boldsymbol{u}_Q]^T \boldsymbol{y}(t)$$

ブレインノイズの影響を効率よく除去できるものの，Qの決定が難しい.

Auditory evoked field

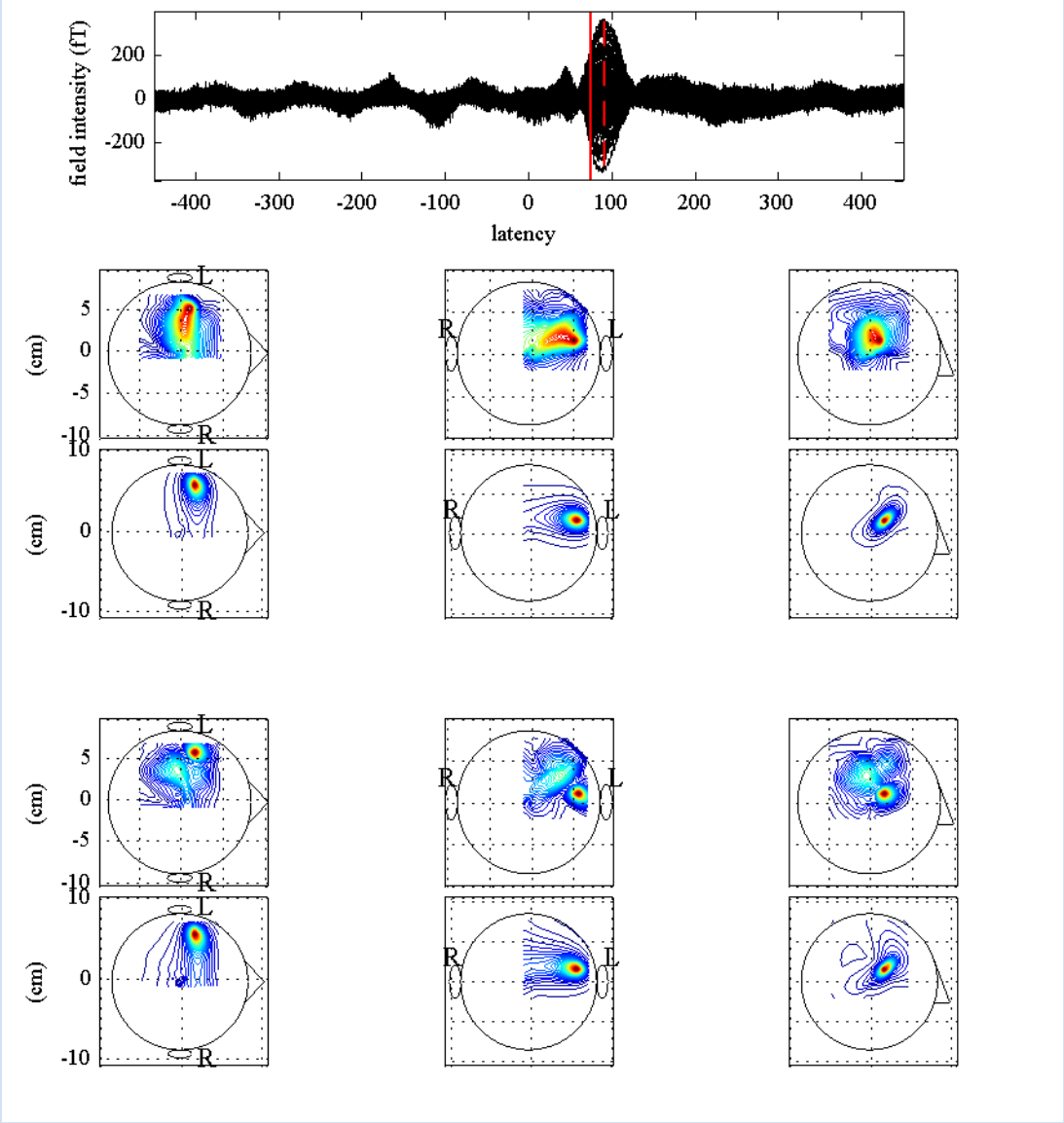

73ms

Conventional

Prewhitening

90ms

Conventional

Prewhitening

参考文献

Prewhitening beamformerについては
「Adaptive spatial filter..」の第8章で議論されている．また，以下の2報の論文がオリジナル論文である．

IEEE TRANSACTIONS ON BIOMEDICAL ENGINEERING, VOL. 53, NO. 9, SEPTEMBER 2006 1755

A Novel Adaptive Beamformer for MEG Source Reconstruction Effective When Large Background Brain Activities Exist

Kensuke Sekihara*, *Senior Member, IEEE*, Kenneth E. Hild, II, *Senior Member, IEEE*, and Srikantan S. Nagarajan, *Member, IEEE*

***Abstract*—This paper proposes a novel prewhitening eigenspace beamformer suitable for magnetoencephalogram (MEG) source reconstruction when large background brain activities exist. The prerequisite for the method is that control-state measurements, which contain only the contributions from the background interference, be available, and that the covariance matrix of the background interference can be obtained from such control-state measurements. The proposed method then uses this interference covariance matrix to remove the influence of the interference in the reconstruction obtained from the target measurements. A numerical example, as well as applications to two types of MEG data, demonstrates the effectiveness of the proposed method.**

***Index Terms*—Adaptive beamforming, brain noise, magnetoencephalography, prewhitening, source reconstruction.**

background
method is tha
the contribut
able, and tha
ference can b
The proposed
trix to remov
tion results o
signal and in
The propo
structing sou
time-locked

1112 IEEE TRANSACTIONS ON BIOMEDICAL ENGINEERING, VOL. 55, NO. 3, MARCH 2008

Performance of Prewhitening Beamforming in MEG Dual Experimental Conditions

Kensuke Sekihara*, Kenneth E. Hild, II, *Senior Member, IEEE*, Sarang S. Dalal, and Srikantan S. Nagarajan, *Senior Member, IEEE*

***Abstract*—This paper presents an analysis on the performance of the prewhitening beamformer when applied to magnetoencephalography (MEG) experiments involving dual (task and control) conditions. We first analyze the method's robustness to two types of violations of the prerequisites for the prewhitening method that may arise in real-life two-condition experiments. In one type of violation, some sources exist only in the control condition but not in the task condition. In the other type of violation, some signal sources exist both in the control and the task conditions, and that they change intensity between the two conditions. Our analysis shows that the prewhitening method is very robust to these nonideal conditions. In this paper, we also present a theoretical analysis showing that the prewhitening method is**

under these two conditions is a common procedure to reconstruct signal sources of interest [1]. (This subtraction is often performed as a part of calculating pseudo-t statistics, which is used for statistically evaluating the source configuration difference between the two conditions.) However, when the source reconstruction is performed with adaptive spatial filter methods [2]–[4], such subtraction-based methods cannot effectively remove the influence of the background interference [5]. This is because the influence of the background activity is not simply additive. It involves spatial blur and source location bias, as will be shown in our computer simulation in Section V.

自発脳磁界解析への応用：

刺激に対してロックしていない脳活動（Induced activity）の検出と解析

Induced activity

Task-related modulation of oscillatory brain activity
（タスクによって引き起こされる脳律動の変調成分）

Induced activity:

- Stimulus-evoked but not phase-locked to the stimulus
- frequency specific

↓

Event-related (spectral) power change

Power decrease → Event-related desynchronization (ERD)

Power increase → Event-related synchronization (ERS)

G. Pfurtscheller and F. H. Lopes da Silva: “Event-related EEG/MEG synchronization and desynchronization: basic principles,” Clin. Neurophysiol., 1997

Induced activity may not be detected in averaged results

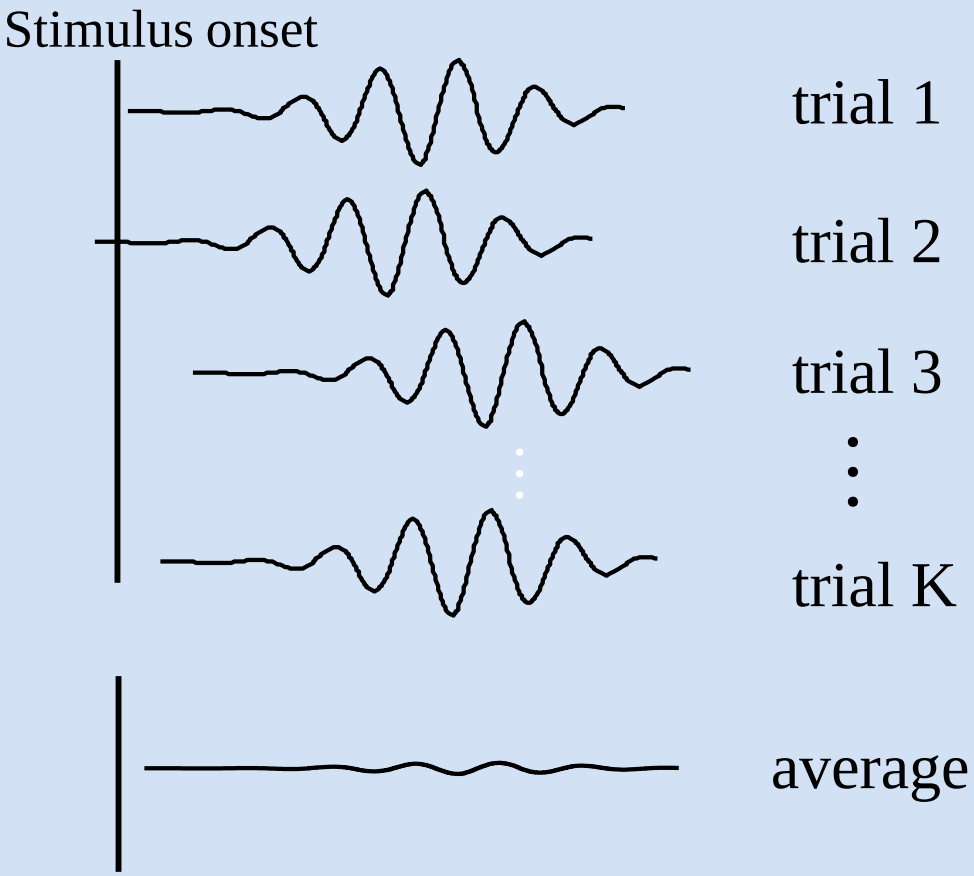

Induced activity has time jitter

Motor-evoked MEG
100-trial-averaged results

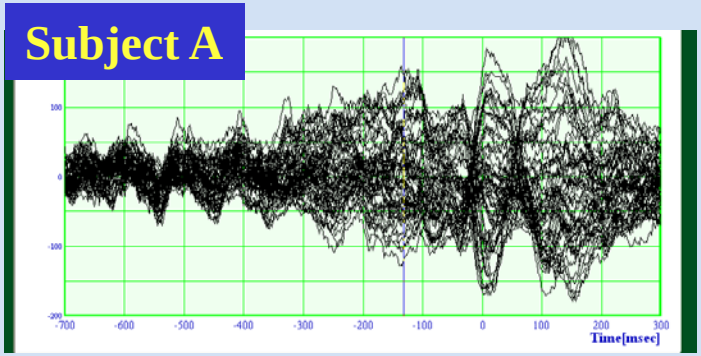

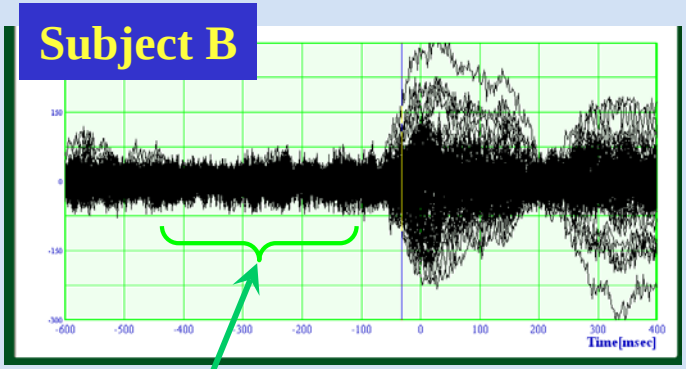

No clear premotor response exists in average waveform

Covariance matrices are computed from non-averaged trials, and averaged across epochs

Stimulus onset

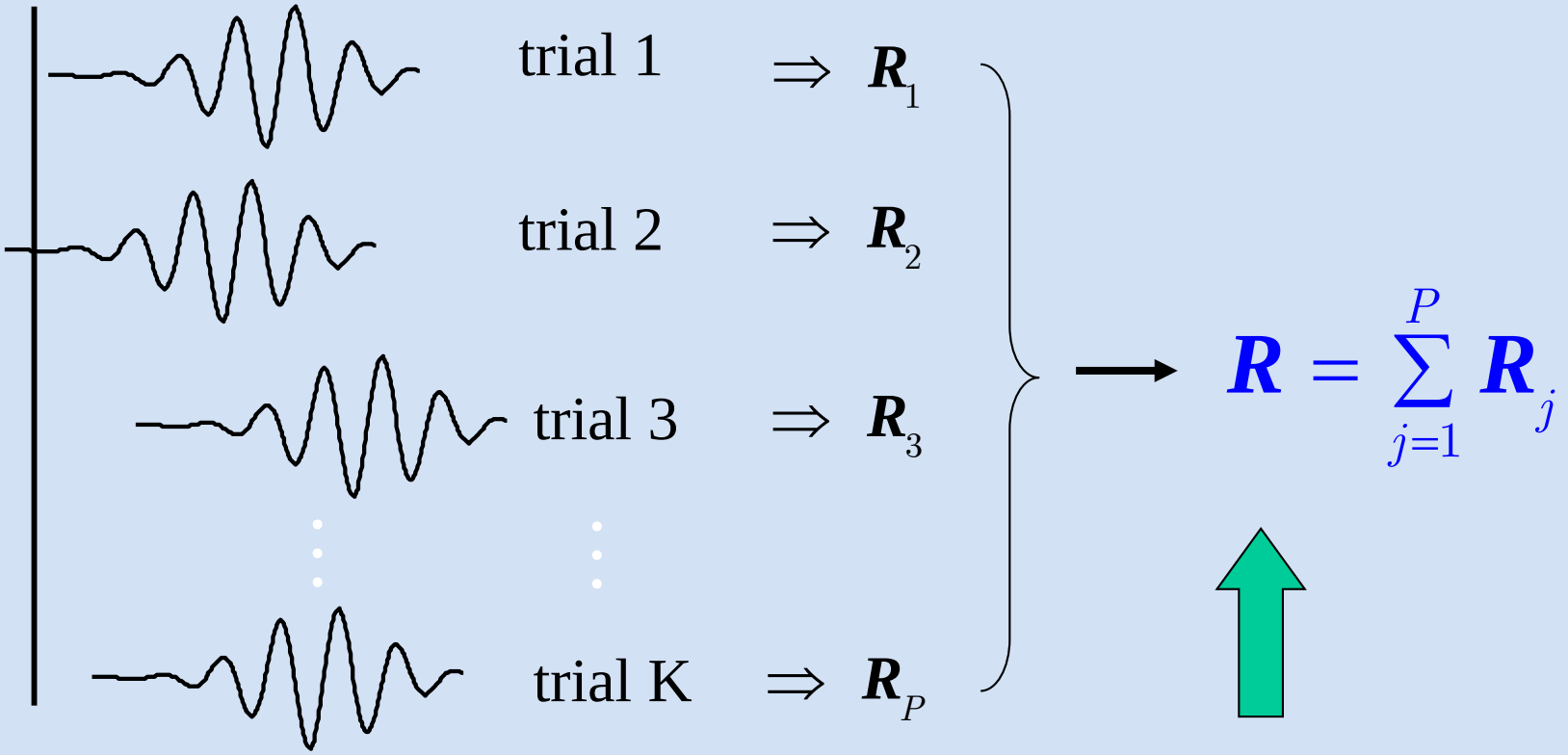

This *R* contains unwanted background interference

Dual-condition experiments

Task: $\boldsymbol{y}(t) = \boldsymbol{y}_S(t) + \boldsymbol{y}_I(t) + \boldsymbol{\varepsilon}$

Control: $\boldsymbol{y}_C(t) = \boldsymbol{y}_I(t) + \boldsymbol{\varepsilon}$

Covariance matrix relations ↓

Task: $\boldsymbol{R} = \boldsymbol{R}_S + \boldsymbol{R}_{i+\varepsilon}$

Control: $\boldsymbol{R}_C = \boldsymbol{R}_{i+\varepsilon}$

Problem:

この場合，$\boldsymbol{y}_S(t)$ および $\boldsymbol{y}_I(t)$ とも自発脳磁解であり，同程度の強度を持つ.

Prewhitening beamforming

Task: $\boldsymbol{R} = \boldsymbol{R}_S + \boldsymbol{R}_{i+\varepsilon}$

Control: $\boldsymbol{R}_C = \boldsymbol{R}_{i+\varepsilon}$

$\Rightarrow$ Calculate $\tilde{\boldsymbol{R}} = \boldsymbol{R}_C^{-1/2} \boldsymbol{R} \boldsymbol{R}_C^{-1/2}$

Signal covariance estimation

$$\hat{\boldsymbol{R}}_S = \boldsymbol{R}_C^{1/2} \left[\boldsymbol{U}_S \boldsymbol{U}_S^T (\tilde{\boldsymbol{R}} - \boldsymbol{I}) \right] \boldsymbol{R}_C^{1/2} = \boldsymbol{R}_C^{1/2} \left[\sum_{j=1}^{Q} \gamma_j \boldsymbol{u}_j \boldsymbol{u} \right] \boldsymbol{R}_C^{1/2}$$

$\boldsymbol{U}_S = [\boldsymbol{u}_1, \ldots, \boldsymbol{u}_Q] : \tilde{\boldsymbol{R}}$ の信号レベル固有ベクトル

$\boldsymbol{y}_S(t)$ および $\boldsymbol{y}_I(t)$ とも自発脳磁解であり，同程度の強度を持つため，

Q を決めることが難しい．（$\tilde{\boldsymbol{R}}$ の固有値スペクトルは明瞭な閾値を持たない）

Robinson's *F* ratio method

Define $s(\boldsymbol{r},t)$: source image from $\boldsymbol{y}(t)$

$s_C(\boldsymbol{r},t)$: source image from $\boldsymbol{y}_C(t)$

$$\boldsymbol{R}_{total} = \boldsymbol{R} + \boldsymbol{R}_C$$

$$\hat{s}(\boldsymbol{r},t) = \frac{\boldsymbol{l}^T(\boldsymbol{r})\boldsymbol{R}_{total}^{-1}\boldsymbol{y}(t)}{\boldsymbol{l}^T(\boldsymbol{r})\boldsymbol{R}_{total}^{-1}\boldsymbol{l}(\boldsymbol{r})} \quad \text{and} \quad \hat{s}_C(\boldsymbol{r},t) = \frac{\boldsymbol{l}^T(\boldsymbol{r})\boldsymbol{R}_{total}^{-1}\boldsymbol{y}_C(t)}{\boldsymbol{l}^T(\boldsymbol{r})\boldsymbol{R}_{total}^{-1}\boldsymbol{l}(\boldsymbol{r})}$$

$$F(\boldsymbol{r}) = \frac{\left\langle s(\boldsymbol{r},t)^2 \right\rangle - \left\langle s_C(\boldsymbol{r},t)^2 \right\rangle}{\left\langle s_C(\boldsymbol{r},t)^2 \right\rangle}$$

S. E. Robinson and J. Vrba, Recent Advances in Biomagnetism, pp. 302-305, 1999

Frequency-domain beamformer (Narrow-band beamforming)

Because the induced signal is frequency specific, another strategy that further reduces the brain-noise-influence is to use the weight tuned to the frequency of the induced signal.

Frequency-specific weight (Narrow-band weight)

$$\boldsymbol{R}(f) = \left\langle \boldsymbol{\Gamma}(f)\boldsymbol{\Gamma}^{H}(f) \right\rangle \text{ where } \boldsymbol{y}(t) \xleftrightarrow[F.T.]{} \boldsymbol{\Gamma}(f)$$

$$\boldsymbol{w}(\boldsymbol{r}, f) = \boldsymbol{R}(f)\, \boldsymbol{l}(\boldsymbol{r}) \,/\, [\boldsymbol{l}^{T}(\boldsymbol{r})\boldsymbol{R}(f)\, \boldsymbol{l}(\boldsymbol{r})]$$

$\boldsymbol{R}(f)$: Cross-spectral matrix calculated from the frequency band of the induced signal.

Time-frequency-domain beamformer

Time-frequency-specific weight

$$\boldsymbol{y}(t) \xleftrightarrow[\text{Windowed F.T.}]{} \boldsymbol{\Gamma}(\tau, f)$$

Induced activityが含まれている時間周波数領域の中心時間をτ, 中心周波数をfとすれば：

$$\boldsymbol{R}(\tau, f) = \left\langle \boldsymbol{\Gamma}(\tau, f)\boldsymbol{\Gamma}^{H}(\tau, f) \right\rangle$$

$$\boldsymbol{w}(\boldsymbol{r}, \tau, f) = \boldsymbol{R}(\tau, f)\, \boldsymbol{l}(\boldsymbol{r}) \,/\, [\boldsymbol{l}^{T}(\boldsymbol{r})\boldsymbol{R}(\tau, f)\, \boldsymbol{l}(\boldsymbol{r})]$$

ここで，記号 $\langle \cdot \rangle$ はエポックでのアベレージを表す．連続的に計測した自発脳磁解をエポック化し，エポックでのアベレージを計算する

Results of frequency-specific-prewhitening filter for hand-motor measurement

Voluntary right-finger movement (every 10 sec)

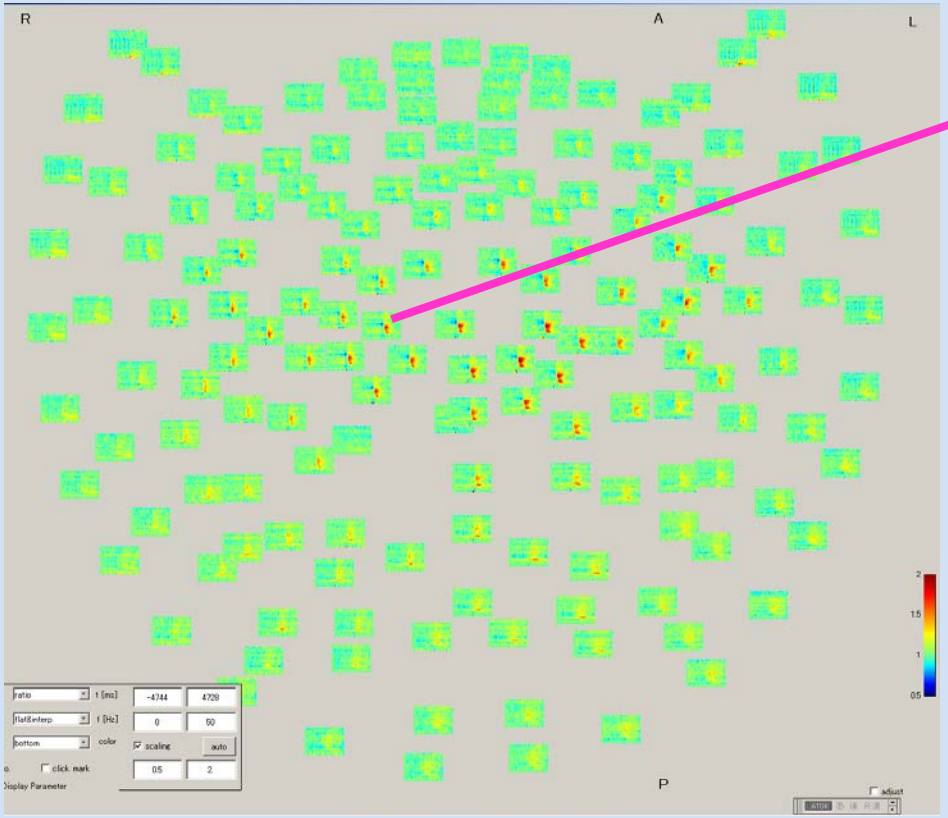

TF maps of data from all sensors

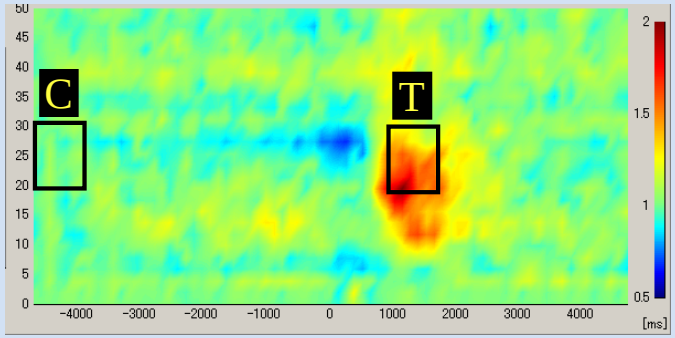

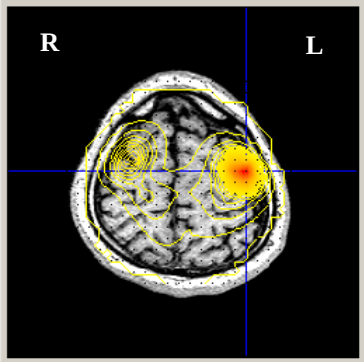

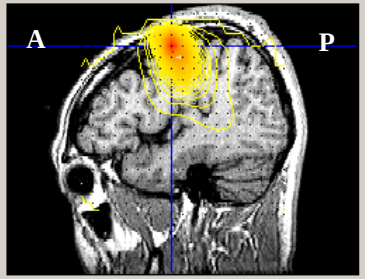

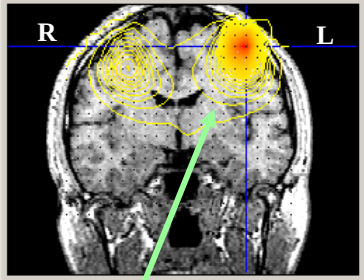

A localized source is found near contra-lateral M1 area

Comparison between prewhitening and F-image methods

MRI overlay

Prewhitening results

F image results

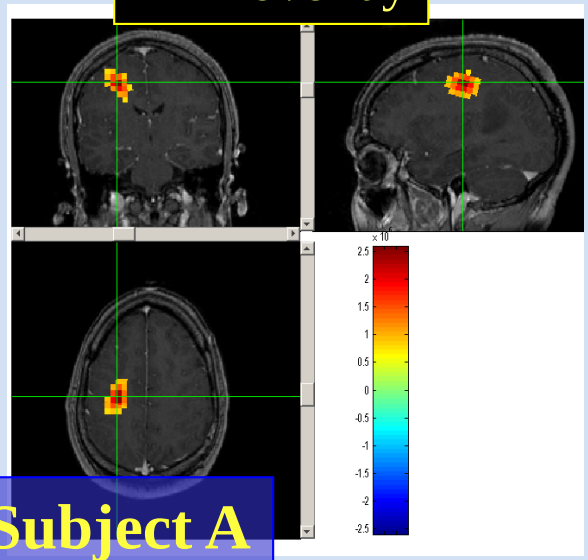

Subject A

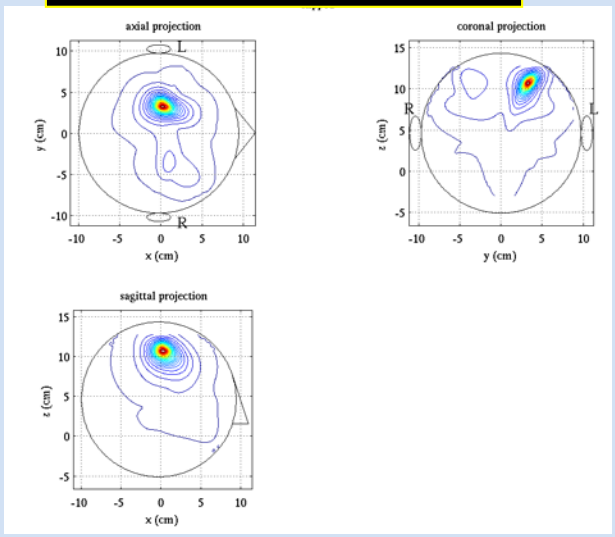

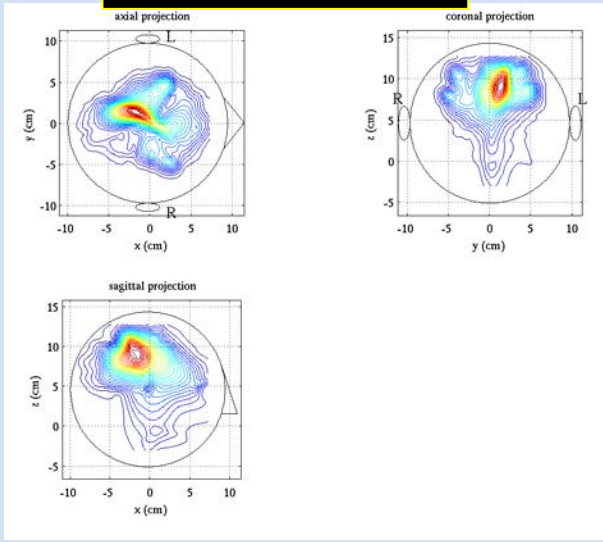

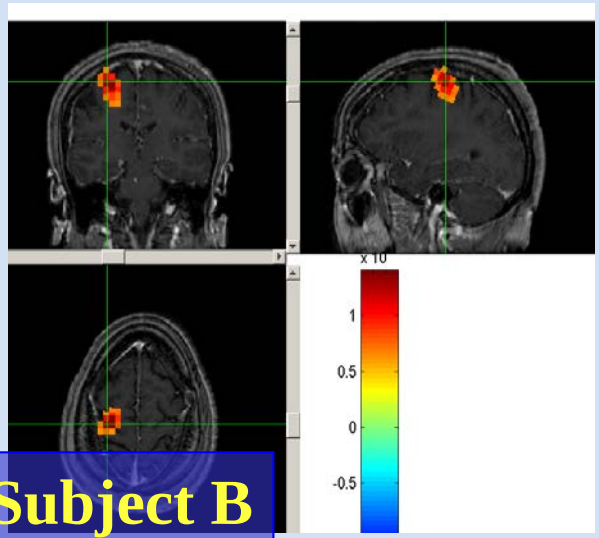

Subject B

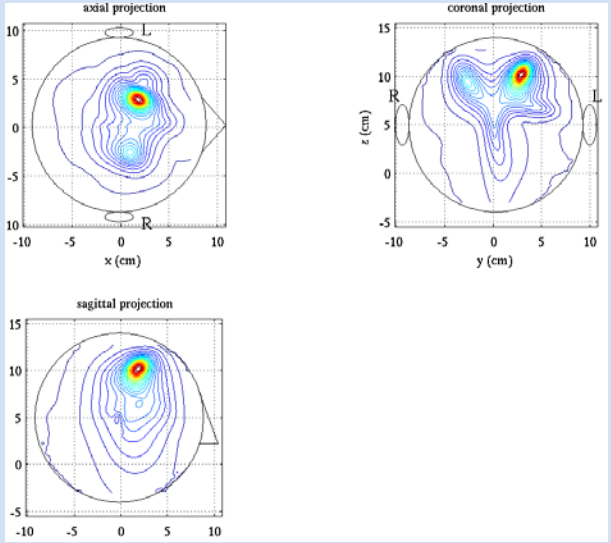

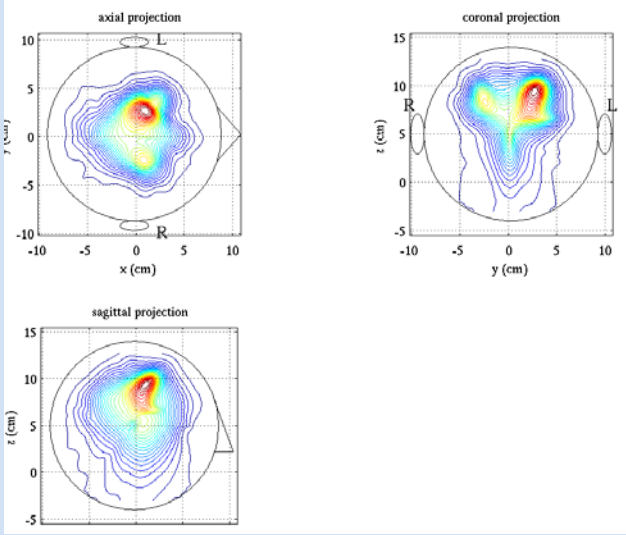

Spike-locked dual-state adaptive spatial filter

発作間欠期のてんかん性スパイクの信号源推定をベータおよびガンマ帯のパワーチェンジから行う.

60分のcontinuous resting state MEGからスパイクを含む複数個のデータ部位を選び出す.

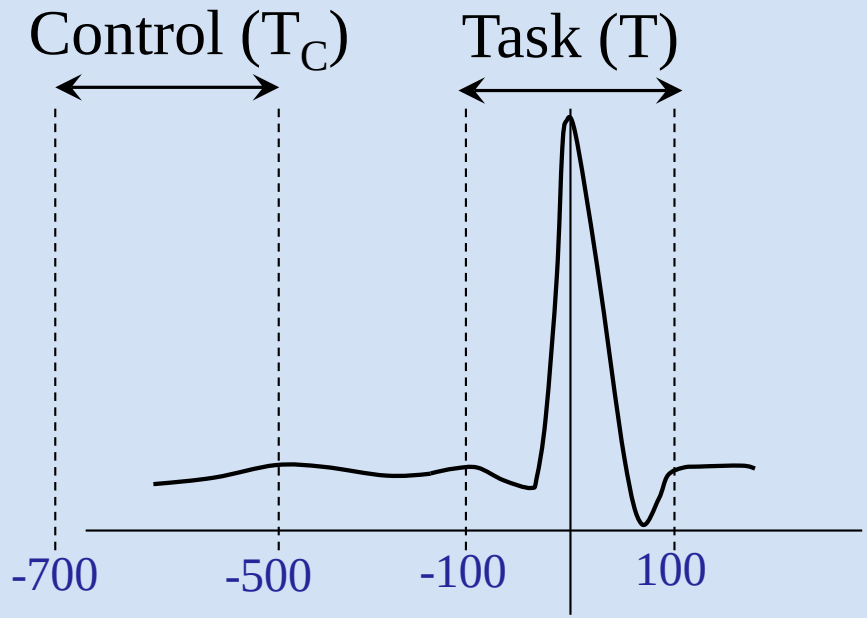

ControlとTask共分散行列を以下のように計算

$$\boldsymbol{R}_C = \sum_{\text{spikes}} \sum_{f \in F_W} \boldsymbol{R}(f, T_C)$$

$$\boldsymbol{R} = \sum_{\text{spikes}} \sum_{f \in F_W} \boldsymbol{R}(f, T)$$

F_W :12-55Hz

A. G. Guggisberg *et al*., NeuroImage Vol.39, 2008

Results from patients #1

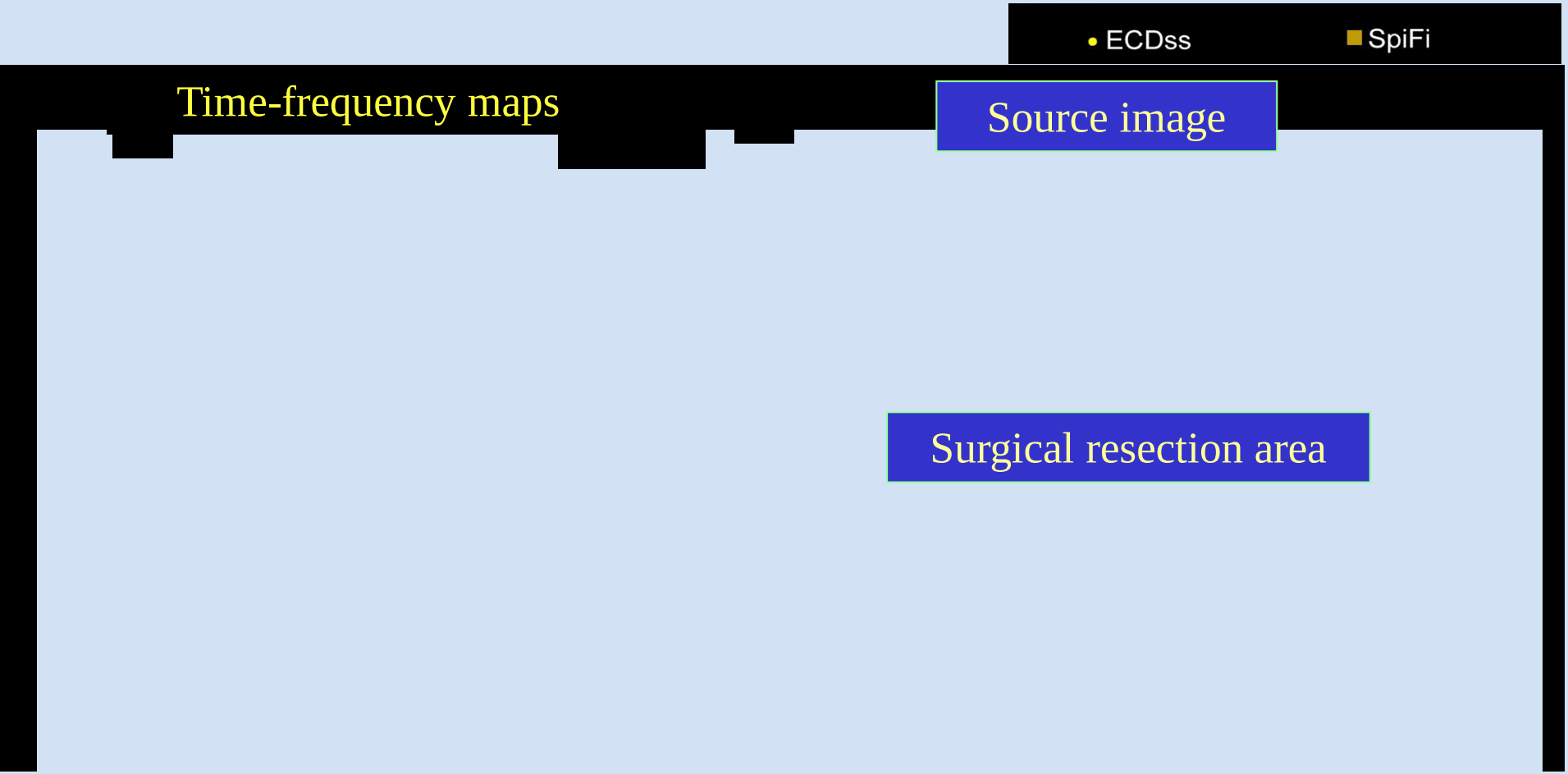

外科的切除部位はMEGのみでなく，他の検査も併用し総合的に決められる．したがって切除部位がてんかん性スパイクの信号源位置推定の「正解」を与えると考え，切除部位と信号源推定結果を比較することで，信号源推定の正しさを評価する．

Results from patients #2

この患者の場合にはbeamformerの結果は外科的切除部位と一致しているが，ダイポールクラスターの位置は切除部位の位置からは大きく外れている

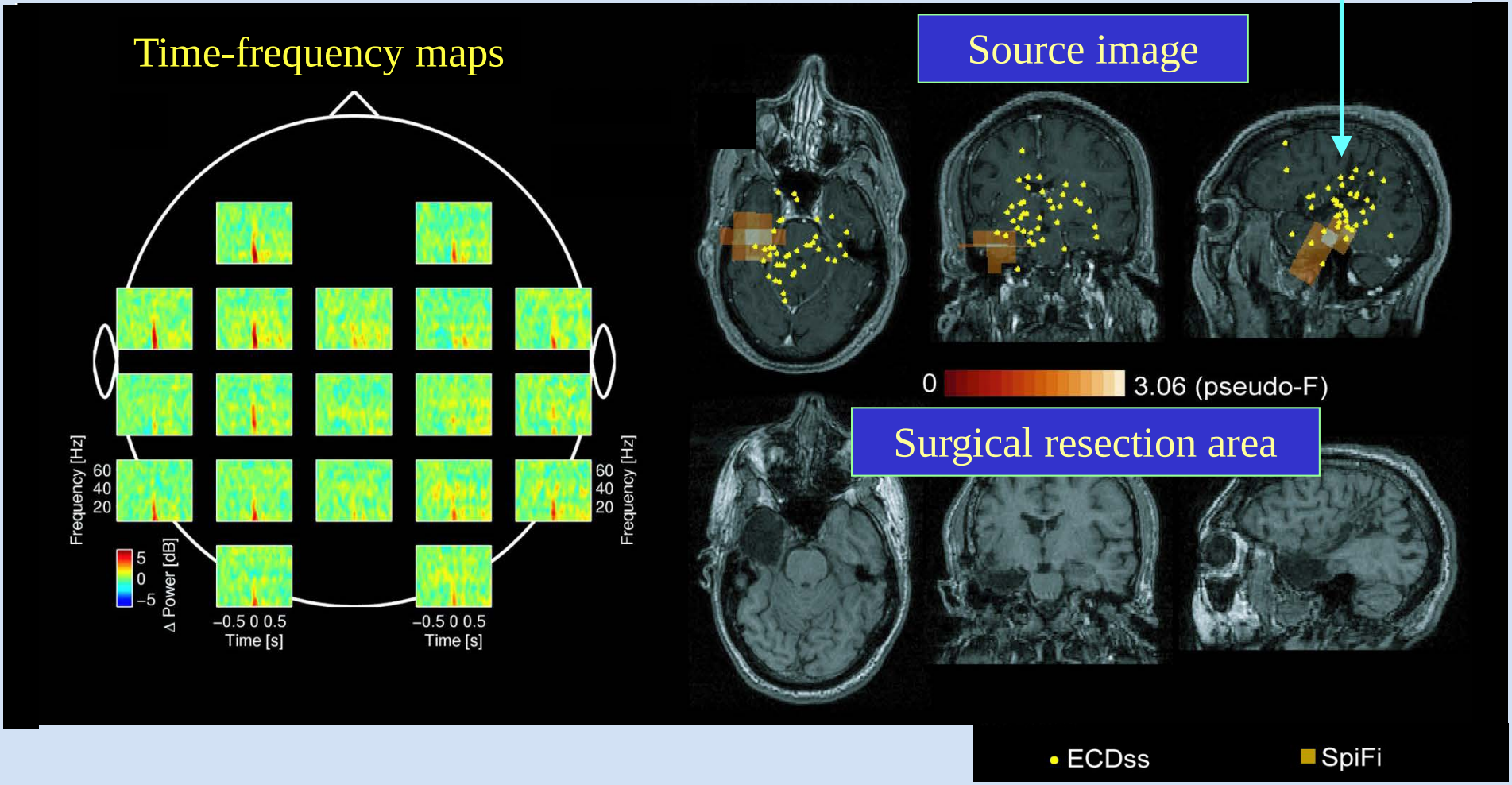

Dual-state spatial filter をさらに拡張することで，時間周波数領域全体に対して信号源再構成が可能となる

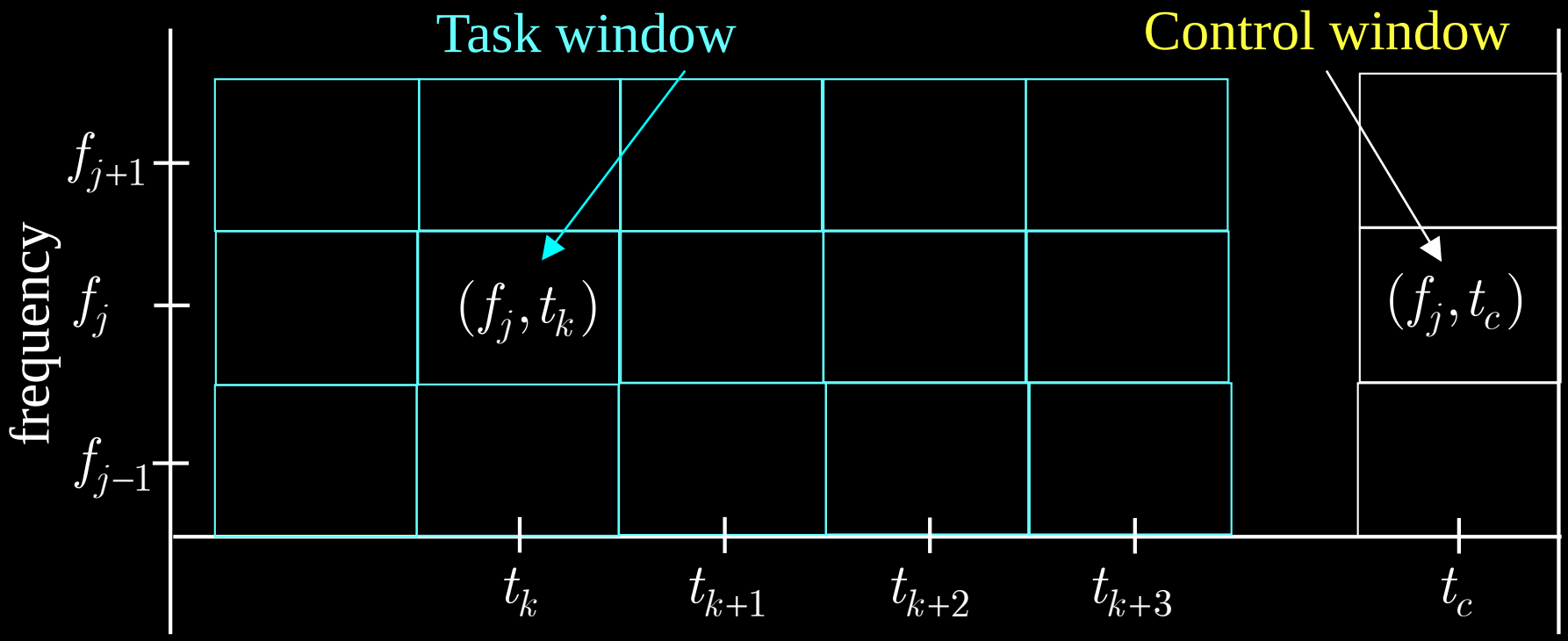

$s(\boldsymbol{r}, f_j, t_k)$：時間周波数領域 (f_j, t_k) に対する再構成結果

A set of $s(\boldsymbol{r}, f_j, t_k)$: $j = 1, 2, \ldots : k = 1, 2, \ldots$ represents time-frequency reconstruction of source activity.

Five dimensional imaging from hand-motor data

Beta-band activity

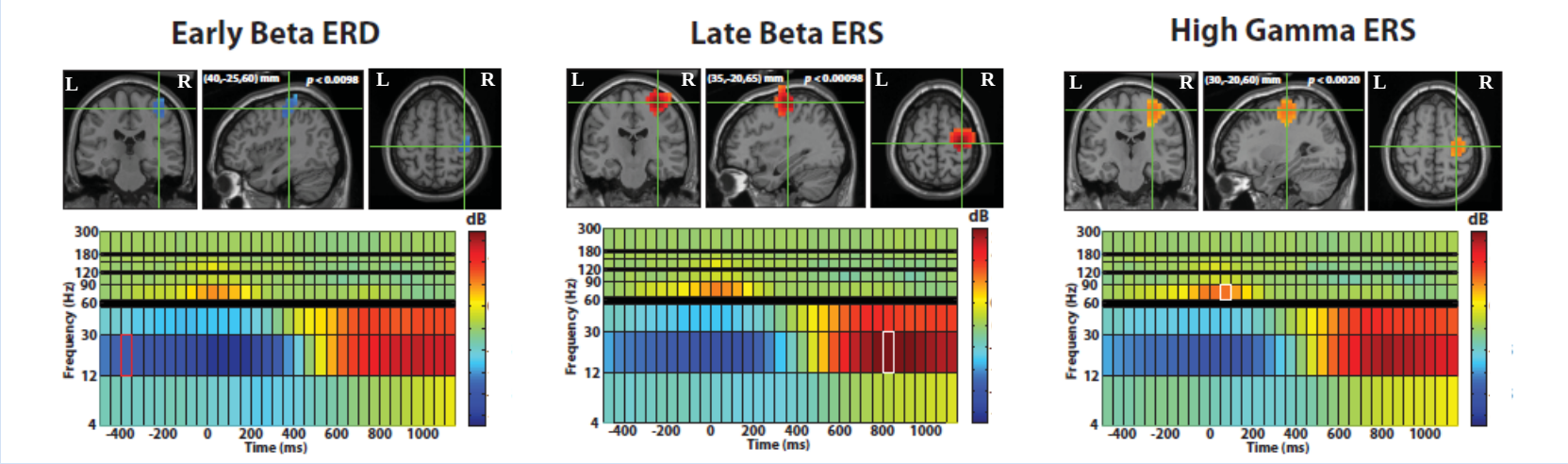

High-gamma-band activity

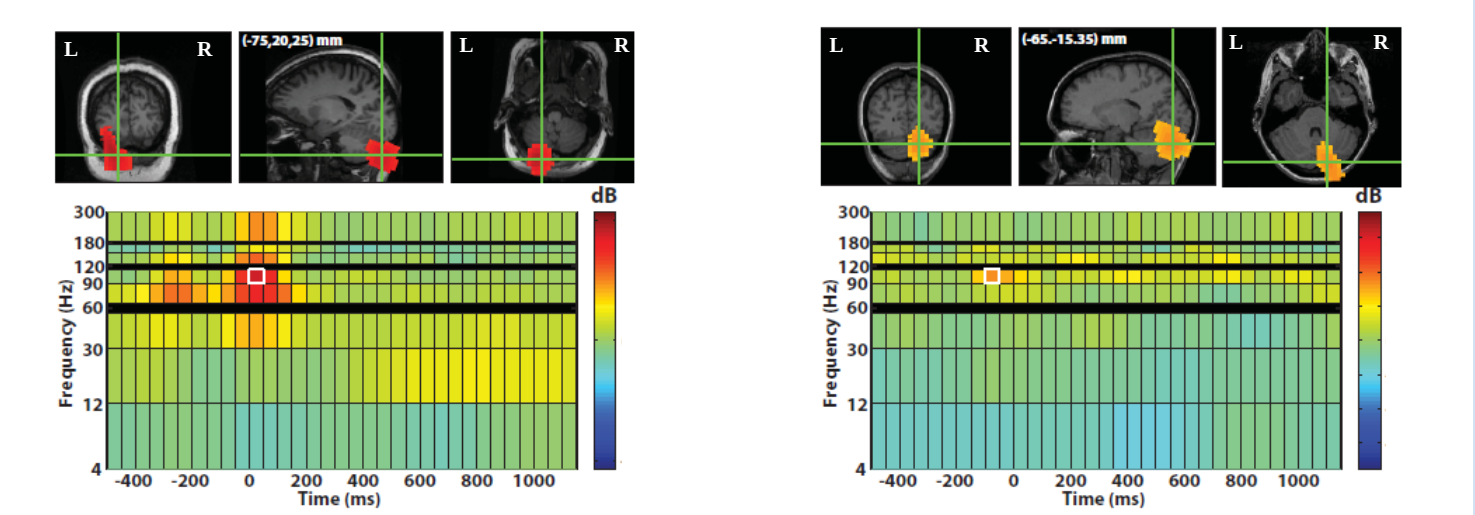

Comparison with ECoG results

Right finger (RD2) movement

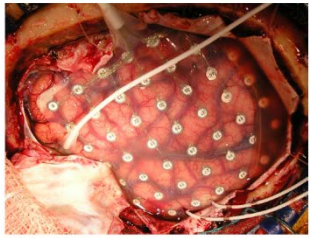

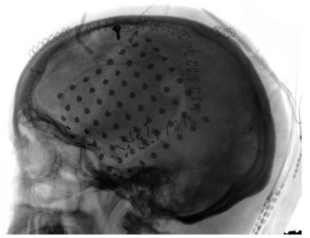

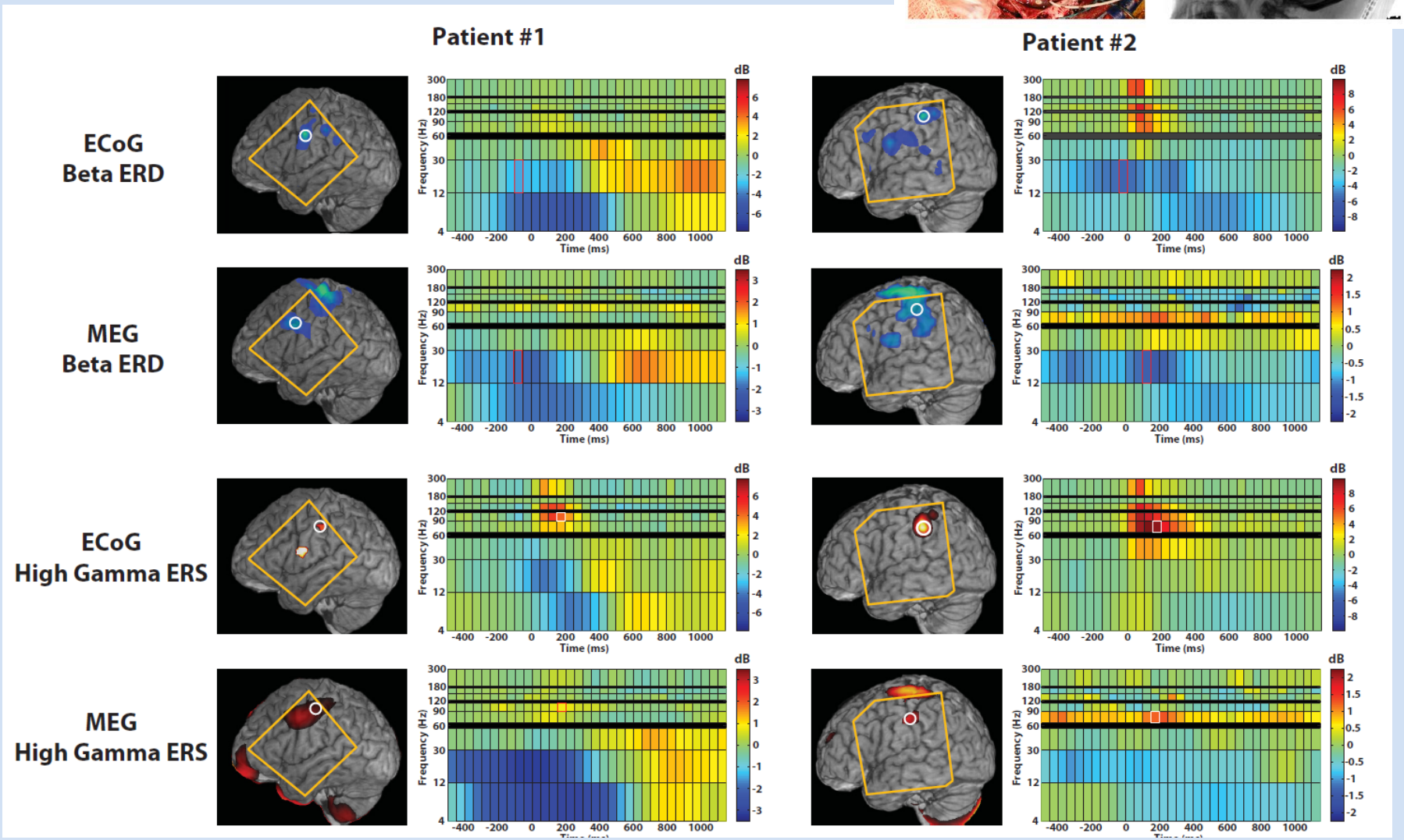

Time-frequency beamformingについては以下の論文に詳細な記載がある.

ELSEVIER

NeuroImage

www.elsevier.com/locate/ynimg
NeuroImage 40 (2008) 1686–1700

Five-dimensional neuroimaging: Localization of the time–frequency dynamics of cortical activity

Sarang S. Dalal,[a,b] Adrian G. Guggisberg,[a,g] Erik Edwards,[a,e] Kensuke Sekihara,[f] Anne M. Findlay,[a] Ryan T. Canolty,[e] Mitchel S. Berger,[c] Robert T. Knight,[e] Nicholas M. Barbaro,[c,d] Heidi E. Kirsch,[d] and Srikantan S. Nagarajan[a,b,*]

[a]*Biomagnetic Imaging Laboratory, Department of Radiology, University of California, San Francisco, CA 94143-0628, USA*
[b]*Joint Graduate Group in Bioengineering, University of California, San Francisco and University of California, Berkeley, USA*
[c]*Department of Neurological Surgery, University of California, San Francisco, CA 94143-0112, USA*
[d]*Department of Neurology, University of California, San Francisco, CA, 94143-0138, USA*
[e]*Helen Wills Neuroscience Institute and Department of Psychology, University of California, Berkeley, CA 94720-3190, USA*
[f]*Department of Systems Design and Engineering, Tokyo Metropolitan University, Tokyo 191-0065, Japan*
[g]*Department of Neurology, University of Bern, Inselspital, 3010 Bern, Switzerland*

Received 28 March 2007; revised 8 January 2008; accepted 17 January 2008
Available online 31 January 2008